

DRAFT VERSION MAY 27, 2021  
Typeset using **LATEX** **manuscript** style in AASTeX63

## The Rotationally Resolved Infrared Spectrum of TiO and Its Isotopologues

DANIEL WITSCH,<sup>1</sup> ALEXANDER A. BREIER,<sup>1</sup> EILEEN DÖRING,<sup>1</sup> KOICHI M. T. YAMADA,<sup>2</sup>  
THOMAS F. GIESEN,<sup>1</sup> AND GUIDO W. FUCHS<sup>1</sup>

<sup>1</sup>*University of Kassel, Institute of Physics, Heinrich-Plett Str. 40, 34132 Kassel, Germany*

<sup>2</sup>*National Metrology Institute of Japan (NMIJ), AIST, Tsukuba 305-8563, Japan*

### ABSTRACT

In this study, we present the ro-vibrationally resolved gas-phase spectrum of the diatomic molecule TiO around  $1000\text{ cm}^{-1}$ . Molecules were produced in a laser ablation source by vaporizing a pure titanium sample in the atmosphere of gaseous nitrous oxide. Adiabatically expanded gas, containing TiO, formed a supersonic jet and was probed perpendicularly to its propagation by infrared radiation from quantum cascade lasers. Fundamental bands of  $^{46-50}\text{TiO}$  and vibrational hotbands of  $^{48}\text{TiO}$  are identified and analyzed. In a mass-independent fitting procedure combining the new infrared data with pure rotational and electronic transitions from the literature, a Dunham-like parameterization is obtained. From the present data set, the multi-isotopic analysis allows to determine the spin-rotation coupling constant  $\gamma$  and the Born-Oppenheimer correction coefficient  $\Delta_{\text{U}_{10}}^{\text{Ti}}$  for the first time. The parameter set enables to calculate the Born-Oppenheimer correction coefficients  $\Delta_{\text{U}_{02}}^{\text{Ti}}$  and  $\Delta_{\text{U}_{02}}^{\text{O}}$ . In addition, the vibrational transition moments for the observed vibrational transitions are reported.

Corresponding author: Daniel Witsch, Guido W. Fuchs  
[d.witsch@physik.uni-kassel.de](mailto:d.witsch@physik.uni-kassel.de)  
[fuchs@physik.uni-kassel.de](mailto:fuchs@physik.uni-kassel.de)

*Keywords:* spectroscopy — high-resolution — infrared — ro-vibrational — titanium monoxide — isotopologues — hotbands

## 1. INTRODUCTION

Since 1904, when the British astronomer Alfred Fowler (1868-1940) showed similarities between the spectra of Antarian stars<sup>1</sup> and the arc spectrum of titanium oxide (TiO), TiO has become a molecule of astrophysical relevance (Fowler 1904). In the second half of the 20<sup>th</sup> century, the blue-green emission in late-type stars were assigned to electronic transitions of TiO by Merrill et al. (1962). Since 1973, the strength of the prominent VIS-UV lines of TiO in spectra of late-type stars are used to classify stars within the Morgan-Keenan spectral classification scheme (Morgan & Keenan 1973). In rare cases, emission bands of TiO can be found in optical spectra of warm circumstellar environments (Barnbaum et al. 1996; Kamiński et al. 2010). Metal oxides, like TiO, are thought to play an important role in the change of the VIS-UV apparent magnitude in Mira-type variable stars at optical as well as infrared wavelengths, as has been demonstrated by Reid & Goldston (2002).

Up to now, TiO signatures in stellar spectra are the topic of many observational studies. Chavez & Lambert (2009) detected isotopologues of TiO towards local M-dwarf stars, such as GJ699 or GJ701, at optical wavelengths. The derived isotopic abundances in these objects are similar to the natural abundance found on earth. Kamiński et al. (2013) detected pure rotational transitions from TiO towards the oxygen-rich late-type star VY Canis Majoris for the first time using the submillimeter array (SMA) between 279.1 GHz and 335.1 GHz. In a follow-up study towards Mira (*o*-Ceti) at submm-wavelength, the detection of all stable titanium isotopologues was reported, with the exception of <sup>47</sup>TiO (Kamiński et al. 2017). In these studies it was shown, that the titanium-bearing molecules, TiO and TiO<sub>2</sub>, are found outside the dust forming regions. From the high abundance, the authors concluded that a substantial fraction of titanium is present as gas-phase species and not as solid dust grains. This is an indication that titanium oxides do not initiate the dust formation - as

<sup>1</sup> i.e. the spectrum of stars like Antares,  $\alpha$  Herculis or *o* Ceti

previously believed. The authors added that titanium might still support the formation of silicate dust. Recently, pure rotational transitions of vibrationally excited TiO were identified towards the AGB stars R Dor and IK Tau by [Danilovich et al. \(accepted 2020\)](#).

First evidence for signs of TiO in atmospheres of extrasolar planets (exoplanets) were found in the atmosphere of the ultra-hot jupiter WASP-121b ([Evans et al. 2016](#)), while earlier studies indicated no presence of TiO in the atmosphere of other investigated exoplanets ([Huitson et al. 2013; Sing et al. 2013](#)). TiO is proposed to contribute to thermal inversion in the atmospheres of hot Jupiters, which is in good agreement with self-consistent atmospheric models [Piette et al. \(2020\)](#). Recently, an improved TiO line list was added to the ExoMol database ([Tennyson et al. 2016; McKemmish et al. 2019](#)), which contains molecules associated with atmospheres of exoplanets. Based on this line list, [Pavlenko et al. \(2020\)](#) investigated the spectra of the M dwarfs GJ15A and GJ15B, revealing non-solar isotopic titanium ratios deduced from synthetic spectra of the TiO isotopologues. Using the Spitzer (IR) Space Telescope, [Smolders et al. \(2012\)](#) published a paper, where they assigned an infrared emission band of the S-type star NP Aurigae to TiO. The spectrum was taken at a resolution of  $2\text{ cm}^{-1}$  and no individual ro-vibrational transitions could be resolved. In the same work, further candidates of TiO emission bands were suggested in the spectra of RX Psc and V899 Aql, but could not be verified.

In terms of laboratory investigations, TiO has been intensivly studied in various experiments. An overview of the works targeting the main isotopologue  $^{48}\text{Ti}^{16}\text{O}$  is given by [McKemmish et al. \(2017\)](#). In the early stages, TiO was commonly produced from modulated high-voltage arc discharge sources, like in the work of [Phillips \(1950\)](#). J. Phillips identified the  $^1\Pi - ^1\Delta$  and the  $^1\Phi - ^1\Delta$  bands of the main isotopologue of TiO in the spectra using a grating spectrograph. Initially, it was mistakenly assumed that the triplet electronic state  $^3\Pi$  is the ground-state ([Lowater 1929; Phillips 1951](#)). In 1969, the  $^3\Delta$  state was correctly assigned as electronic ground-state ([Phillips 1969](#)). Fletcher et al. (1993) investigated the hyperfine splitting of  $^{47}\text{TiO}$ , that originates from the  $I = 5/2$  spin of the rare titanium isotope, using laser induced fluorescence spectra from the  $^3\Pi - ^3\Delta$  transition. Amiot et al. (1995, 1996) performed crossed beam experiments between a molecular beam of TiO and

a continuous wave tunable laser to study the  $^3\Pi - ^3\Delta$  and the  $^1\Phi - ^1\Delta$  bands at sub-Doppler resolution. The laser induced fluorescence spectra led to a comprehensive determination of the rotational molecular constants, as well as spin-orbit- and spin-spin-coupling constants,  $A$  and  $\lambda$ . A few years later, two bands,  $^3\Phi - ^3\Delta$  and  $^1\Pi - ^1\Delta$  of the TiO main isotopologue, were identified in sunspots by Ram et al. (1996, 1999). This observation was based on laboratory measurements conducted between 10,000 and 16,000 cm<sup>-1</sup>, where TiO was produced using a hollow cathode lamp. The same authors also improved the  $^3\Delta$  ground-state rotational constants of  $^{48}\text{TiO}$  by including pure rotational transitions from jet cooled-measurements. Namiki & Ito (2002) and Namiki et al. (2003, 2004) analyzed several vibronic transitions of  $^{48}\text{TiO}$  of the  $^3\Delta$  electronic ground-state in the optical frequency range. Measurements of the  $^3\Pi - ^3\Delta$  transition of all TiO isotopologues in a jet-cooled experiment were performed by Kobayashi et al. (2002). Pure rotational transitions of laser ablated TiO were measured by Kania et al. (2008) in a supersonic-jet expansion utilizing millimeter-wave spectroscopy. Recently, Lincowski et al. (2016) presented a spectroscopic analysis of the rare isotopologues of TiO by means of high-resolution millimeter/submillimeter spectroscopy. From this study hyperfine constants of  $^{47}\text{TiO}$  and  $^{49}\text{TiO}$  were determined. The results agree well with those obtained by Fletcher et al. (1993). Lincowski et al. (2016) also obtained rotational constants, including centrifugal distortion constants for spin-spin and spin-orbit parameters, for all stable titanium isotopologues. Breier et al. (2019) conducted measurements for all stable titanium isotopologues of TiO around 300 GHz. The data were analyzed using a mass-independent Dunham approach, which allows to investigate all isotopologues in a global fit, thus combining measurements at microwave and optical wavelengths. In turn, the Dunham analysis allowed to predict frequencies for the radioactive molecule  $^{44}\text{TiO}$  within a sub-MHz uncertainty. This unstable isotopologue decays with a half-life of 60 years and is of particular interest in the context of young supernova remnants (Sieger et al. 2015; Tsygankov et al. 2016; Austin et al. 2017). The titanium isotope  $^{44}\text{Ti}$  is synthesized in core-collapse supernovae during helium burning reactions.

In this study, we present the first measurement of the infrared spectra of TiO and of all stable titanium isotopologues as well as the spectra of the vibrational hotbands of  $^{48}\text{TiO}$ . In total 1034

transitions have been assigned and a line list with data of accuracy better than  $10^{-3}\text{ cm}^{-1}$  was assembled to guide future astronomical observations. Transitions from vibrationally excited states of up to  $v = 3$  have been observed in our experiments. Together with data from the literature (Breier et al. 2019; Lincowski et al. 2016; Fletcher et al. 1993; Ram et al. 1999; Amiot et al. 1995), a mass-independent Dunham analysis, based on that presented in Breier et al. (2019), was performed, which results in new insights into the vibrational potential of TiO.

## 2. EXPERIMENTAL APPROACH

The experiments in this work have been performed using a laser ablation technique combined with a supersonic jet expansion, intersected with infrared radiation from a quantum cascade laser (QCL), see Witsch et al. (2019) for a detailed description of the experimental setup. Here, only a brief description is given. A highly intense laser pulse of 7 ns pulse duration with an output power of up to 33.5 mJ/pulse produced by a Nd:YAG laser from *Continuum Lasers (Inlite II-20 Series)* was focused onto the surface of a pure titanium sample rod and produced a hot titanium plasma ( $\sim 10,000\text{ K}$ ). The sample rod with a diameter of 1 cm and a length of 5 cm containing titanium isotopes in natural abundances (see Table 1) was rotated and translated in order to continuously provide a pristine surface for the ablation processes. A helium buffer gas containing 3 % of nitrous oxide ( $\text{N}_2\text{O}$ ) as an oxygen donor was used as a carrier gas, for picking up parts of the ablated material. A *Parker Series 9 General Valve* was used to produce carrier gas pulses of  $500\text{ }\mu\text{s}$  duration. In a subsequent reaction channel of 4 mm length and  $12\text{ mm} \times 1\text{ mm}$  cross section, TiO was formed and finally adiabatically expanded into a vacuum chamber of  $1.2 \times 10^{-1}\text{ mbar}$  background pressure. As a result, a supersonic jet was formed, which was probed by a quantum cascade laser (QCL) beam perpendicular to its propagation. A Herriott-type multi-pass cell (Herriott et al. 1964) guided the radiation 40 times through the jet to increase the absorption length. The experiment was operated at a repetition rate of 20 Hz. The delay between the gas flow and the ablation laser pulse was controlled by a trigger pulse generator (*Quantum Composers 9300 series*) to optimize the TiO yield.

In the frequency range between 984 and  $992\text{ cm}^{-1}$ , spectra were measured in a step-scan mode (Witsch et al. 2019), using a narrow linewidth distributed feedback (DFB) QCL (*Alpes Lasers*).

After 40 ablation processes the QCL was stepped by  $1.62 \times 10^{-4} \text{ cm}^{-1}$ . A liquid nitrogen cooled mercury cadmium tellurid (MCT) detector with 300 kHz response was used to record absorption signals of TiO.

Furthermore, experiments were performed between  $971 \text{ cm}^{-1}$  and  $1032 \text{ cm}^{-1}$  using a mode-hop-free external cavity (ec) QCL from *Daylight Solutions*. The infrared radiation was detected by a fast liquid nitrogen cooled 1 GHz-response-MCT detector. By applying a 200 kHz frequency modulation to the ec-QCL, spectral intervals of  $0.03 \text{ cm}^{-1}$  width were acquired 600 times before stepping to the next spectral interval.

All spectra were calibrated by simultaneously measuring the spectrum of an internally coupled etalon with a free spectral range of  $0.006 \text{ cm}^{-1}$  ( $0.01 \text{ cm}^{-1}$  in step scan measurements) and the spectrum of methanol ( $\text{CH}_3\text{OH}$ ) in a Herriott-type multi-pass gas cell. The pressure in the cell was reduced until the Doppler width dominated the line broadening. The reference spectrum was calibrated using line positions from the Hitran database (Xu et al. 2004). The calibration accuracy was better than  $2.8 \times 10^{-4} \text{ cm}^{-1}$ .

### 3. THE IR SPECTRUM OF TiO

In this study, we present the first rotationally resolved infrared spectrum of TiO between  $971.2 \text{ cm}^{-1}$  and  $1031.9 \text{ cm}^{-1}$ , as shown in Figure 1. The laser ablation source does not provide a constant molecular yield, which causes intensity fluctuations in the observed spectrum. A total of 1034 transitions were assigned to the fundamental bands of TiO and its stable titanium isotopologues,  $^{46-50}\text{TiO}$ , as well as vibrational hotbands of the main isotopologue  $^{48}\text{TiO}$ . The typical linewidth is  $2 \times 10^{-3} \text{ cm}^{-1}$  (60 MHz). The band centers are listed in Table 1. A detailed list of transitions is provided in the supplemental material in Tables 5 to 12.

For the main isotopologue,  $^{48}\text{TiO}$ , ro-vibrational transitions in the  $^3\Delta$  electronic ground state of  $J''$  up to 25 and 32 have been assigned to the P- and the R-branch, respectively. In addition, 63 Q-branch transitions were assigned. As listed in Table 1, several hotband transitions of  $^{48}\text{TiO}$  and transitions originating from  $^{46}\text{TiO}$ ,  $^{47}\text{TiO}$ ,  $^{49}\text{TiO}$  and  $^{50}\text{TiO}$  are identified (see Figure 1) and appear in natural abundance. Transitions of  $^{47}\text{TiO}$  (nuclear spin  $I = 5/2$ ) and  $^{49}\text{TiO}$  ( $I = 7/2$ ) with low  $J''$

values exhibit larger linewidths of up to  $2.5 \times 10^{-3} \text{ cm}^{-1}$  (75 MHz), because of the unresolved hyperfine structure. Due to the spin-orbit coupling, energy levels split into three  $\Omega$ -components. Transitions between different  $\Omega$  are prohibited by selection rules, resulting in three transitions for each  $J''$  as can be seen in the upper plot in Figure 1. For  $J'' > 6$  the splitting into three  $\Omega$ -components was observed for all isotopologues. However, as the total angular momentum can not be smaller than its components, only states with  $J \geq \Omega$  exist, thus dissolving the triplet structure for the lowest  $J''$  transitions. Furthermore, for  $J'' \leq 5$ , some  $\Omega = 3$  transitions were too weak to be observed and for the lowest  $J''$  values some  $\Omega = 2$  components could not be detected due to the unfavorable partition function.

Finally, transitions belonging to higher vibrational states ( $v'' \geq 1$ ) of  $^{48}\text{TiO}$  were found in the observed spectrum. In total 3 hotbands were assigned ( $v = 2 \leftarrow 1$ ,  $3 \leftarrow 2$  and  $4 \leftarrow 3$ ) indicating that the vibrational excitation of TiO is not effectively cooled in the supersonic jet expansion – contrary to the rotational excitation. The most populated hotband ( $v = 2 \leftarrow 1$ ) exhibits Q-branch transitions at  $990.9 \text{ cm}^{-1}$ , while the Q-branches from the other hotbands are too weak to be observed in our spectrum.

#### 4. ISOTOPICALLY INVARIANT FITTING PROCEDURE

The energy levels of the diatomic molecules, titanium monoxide and its isotopologues, can be described by the Dunham formalism (Dunham 1932a,b) to obtain a mass-independent molecular parameterization, according to Equation 1. Molecular parameters of TiO were derived from a global data set analysis using high-resolution data from Breier et al. (2019) and the here presented mid-IR measurements on multi-isotopologue ro-vibrational TiO transitions. The mass-independent molecular parameterization is described in detail by Breier et al. (2018, 2019). In short, the parameter description of TiO is obtained by an adjustment procedure of the following isotopically invariant equation of the molecular parameters,

$$X_{v,\alpha} = \sum_k \left\{ \eta \cdot \mu_\alpha^{-\frac{2l+k}{2}} \cdot \left( 1 + \sum_{i=\text{Ti,O}} \frac{m_e}{M_\alpha^i} \Delta_{\hat{O}_{k,l}}^i \right)_{\text{BO}} \cdot \hat{O}_{k,l} \cdot \left( v + \frac{1}{2} \right)^k \right\}. \quad (1)$$

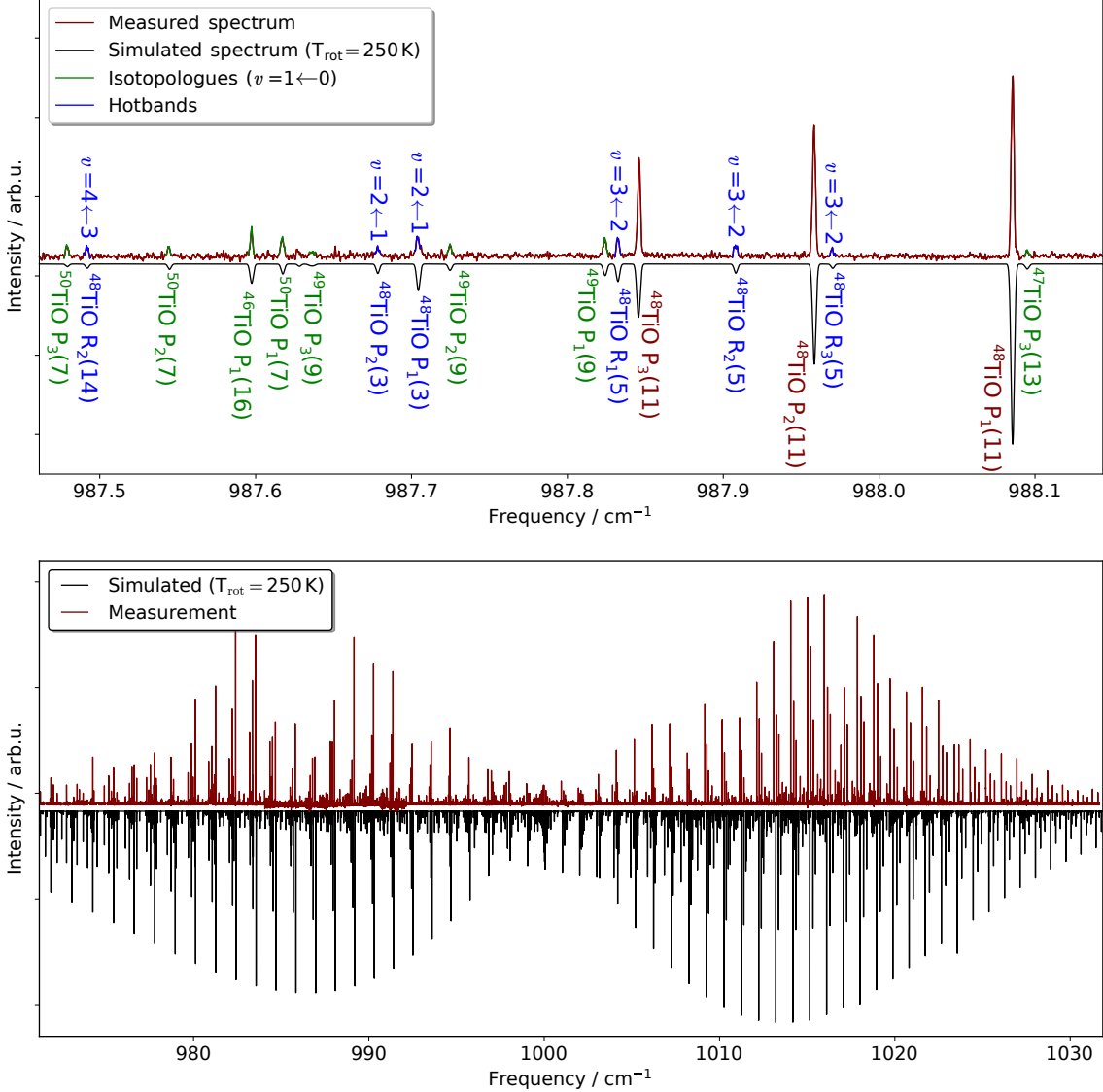


**Figure 1.** The infrared spectrum of TiO. Lower plot: The measured spectrum is shown (upper trace, red) together with a simulated spectrum (lower trace, black) of the fundamental bands of  $^{46-50}\text{TiO}$  and hotbands of  $^{48}\text{TiO}$  up to  $v = 4 \leftarrow 3$  assuming a rotational temperature of 247 K. In the simulation the vibrational temperature is assumed to be 1250 K and the isotopologues are simulated using their natural abundance values (De Laeter et al. 2003). Upper plot: A detailed view of the spectrum around  $987.8\text{ cm}^{-1}$ . The three  $\Omega$  components of the fundamental band of  $^{48}\text{TiO}$  are marked in red, fundamental transitions assigned to the rare isotopologues of TiO are labeled in green. Transitions assigned to the  $^{48}\text{TiO}$  hotbands are labeled in blue. The vibrational quantum numbers for hotband transitions are indicated.

**Table 1.** Number of assigned transitions in the observed spectrum of TiO, its isotopologues, and hot-bands together with measured band centers  $\nu$  and calculated vibrational transition moments. The natural abundance of titanium isotopes is given in percent. A detailed list of transitions is given in Tables 5 to 12.

Isotopologue/	Natural						This work	Ref. <sup>b</sup>
Transition	abundance <sup>a</sup>	$\nu_{i \leftarrow i-1}$ (cm <sup>-1</sup> )	P-branch	Q-branch	R-branch	$ \langle \nu_i   \mu   \nu_{i-1} \rangle $ (D)		
<sup>48</sup> TiO	$v = 1 \leftarrow 0$	73.720(22)	1000.0410(5)	63	47	89	0.230	0.230
	$v = 2 \leftarrow 1$		990.8839(5)	41	32	103	0.323	0.323
	$v = 3 \leftarrow 2$		981.7032(6)	14	0	69	0.393	0.393
	$v = 4 \leftarrow 3$		972.4989(7)	0	0	42	0.452	0.451
<sup>46</sup> TiO	$v = 1 \leftarrow 0$	8.249(21)	1005.4076(5)	73	0	69	—	—
<sup>47</sup> TiO	$v = 1 \leftarrow 0$	7.437(14)	1002.6670(5)	64	0	73	—	—
<sup>49</sup> TiO	$v = 1 \leftarrow 0$	5.409(10)	997.5060(5)	49	0	79	—	—
<sup>50</sup> TiO	$v = 1 \leftarrow 0$	5.185(13)	995.0733(5)	48	0	79	—	—

<sup>a</sup>Values taken from De Laeter et al. (2003)

<sup>b</sup>Values are calculated according to McKemmish et al. (2019) using DUO (Yurchenko et al. 2016)

The isotopic invariant Dunham-like fitting parameter  $\hat{O}_{k,l}$  takes a central role in Equation 1. The index  $l$  describes the expansion of molecular parameters in terms of the angular momentum operator  $\hat{N}^2, \hat{N}^4, \dots, \hat{N}^{2l}$  for the isotopologue  $\alpha$  in its vibrational state  $v$ . For example, the molecular parameters  $B_{v,\alpha}, D_{v,\alpha}$  and  $H_{v,\alpha}$  for  $l = 1, 2, 3$ , respectively, are obtained from the Dunham parameters  $\hat{O}_{k,l} = U_{k,l}$ . The index  $k$  is the ro-vibrational coupling order  $((v + 1/2)^k)$ . In the case of  $l = 1$ , the Dunham parameter  $U_{k,l}$  are linked to the equilibrium rotational constant ( $k = 0$ ) or the rotation-vibration interaction constants ( $k = 1, 2, \dots$ ). Analogous, Dunham-like parameters  $\hat{O}_{k,l}$ , such as  $A_{k,l}, \gamma_{k,l}$  and  $eQq_{0,k,l}$ , are used to describe the fine- and hyperfine-structure, e.g. the spin-orbit coupling constant  $A$ , the spin-rotation coupling constant  $\gamma$  or the electric hyperfine-structure parameter  $eQq_0$ . The coefficient  $\eta$  in Equation 1 is a nucleus scaling factor being unity for rotational and fine-structure parameters. For hyperfine parameters,  $\eta$  is set to be the nuclear  $g_N$ -factor for magnetic hyperfine parameters and the electric hyperfine parameters are scaled by the electric quadrupole moment  $Q$ ,

respectively. The scaling values of TiO are given in Breier et al. (2019). The isotopic invariance is introduced into Equation 1 by the reduced mass  $\mu_\alpha$ . To obtain a more precise description of the mass invariance, the Born-Oppenheimer breakdown (BO) correction is given as sum over parameters  $\Delta_{\hat{O}_{k,l}}^i$ . Its mass dependency is given by the fraction of the electron mass  $m_e$  and the mass of atom  $M_\alpha^i$  ( $i = \text{Ti}, \text{O}$ ). In this work, the BO correction parameters  $\Delta_{\hat{O}_{k,l}}^i$  are determined in addition to the first-order vibrational, rotational and spin-orbital expansion terms  $U_{10}$ ,  $U_{01}$  and  $A_{00}$ , respectively.

In our analysis we used the isotope masses of titanium and oxygen as published by AME2016 (Wang et al. 2017). The generalized equation is implemented in the program PGOPHER (Western 2017). Contrary to Breier et al. (2019), the weighting process of the various data sets is changed and the well-defined iterative re-weighting procedure introduced by Watson (2003) is used to improve the reproducibility. The ROBUST parameter value of PGOPHER was determined to be 0.1.

One advantage of a mass-independent analysis is that the effect of the spin-rotation interaction onto the energy level is distinguishable from the centrifugal distortion of the spin-orbital effects due to their difference in mass scaling behavior (Müller et al. 2015). In this work, two different fitting sets are obtained by excluding the spin-rotation interaction (“Fit A”) or by including this contribution (“Fit B”) in the parameter set. Both parameter sets describe the electronic ground-state ( $X^3\Delta$ ) of TiO with 29 mass-independent Dunham-like molecular parameters, which are shown in Table 2. The confidence of parameter set “Fit B” is emphasized and its usage for TiO is recommended. This Dunham-like parameter set corresponds to 150 effective molecular parameters which describe the vibrational states  $v = 0$  to 4 of  $^{48}\text{TiO}$  and the vibrational states  $v = 0, 1$  of the observed rare isotopologues (including the hyperfine structure of  $^{47}\text{TiO}$  and  $^{49}\text{TiO}$ ). Parameters for the  $A^3\Phi$  and  $B^3\Pi$  state, which are obtained from the global fit, are listed in Tables 13 and 14 of the supplementary material and are not further discussed. The uncertainty of the here measured IR data is  $5.2 \times 10^{-4} \text{ cm}^{-1}$ . The fitting routine within PGOPHER is available on request.

**Table 2.** Mass-invariant molecular parameters for the  $X^3\Delta$  state of TiO based on the analysis of the six stable titanium isotopologues  $^{46-50}\text{Ti}^{16}\text{O}$  and  $^{48}\text{Ti}^{18}\text{O}$ .

Parameter $\hat{O}_{k,l}$	This work		Ref. <sup>a</sup>		Units
	Fit A	Fit B	Fit A	Fit B	
$U_{00}$	0.0	0.0	0.0	0.0	$\text{cm}^{-1}$
$U_{10} \times 10^{-3}$	3.4949905(13)	3.4949915(13)	3.4949966(26)	3.4949959(26)	$\text{cm}^{-1} \text{u}^{1/2}$
$\Delta_{\text{U}_{10}}^{\text{Ti}}$	0.109(31)	0.114(31)	—	—	
$U_{20} \times 10^{-1}$	-5.470311(43)	-5.470315(43)	-5.47093(45)	-5.47063(46)	$\text{cm}^{-1} \text{u}$
$U_{30} \times 10^1$	-1.6302(23)	-1.6300(23)	-1.587(22)	-1.596(22)	$\text{cm}^{-1} \text{u}^{3/2}$
$U_{01}$	6.4227147(57)	6.42351367(72)	6.4227037(25)	6.4234987(74)	$\text{cm}^{-1} \text{u}$
$\Delta_{\text{U}_{01}}^{\text{Ti}}$	-8.397(16)	-8.314(16)	-8.253(24)	-8.282(25)	
$\Delta_{\text{U}_{01}}^{\text{O}}$	-6.116(25)	-9.769(31)	-6.112(8)	-9.722(29)	
$U_{11} \times 10^1$	-1.255794(22)	-1.255799(21)	-1.255825(44)	-1.255631(69)	$\text{cm}^{-1} \text{u}^{3/2}$
$U_{21} \times 10^3$	-1.3339(25)	-1.3337(25)	-1.3467(57)	-1.3542(61)	$\text{cm}^{-1} \text{u}^2$
$U_{02} \times 10^5$	8.67136(21)	8.67227(26)	8.67195(38)	8.67186(38)	$\text{cm}^{-1} \text{u}^2$
$U_{12} \times 10^6$	1.7640(47)	1.7608(47)	1.7341(67)	1.7469(81)	$\text{cm}^{-1} \text{u}^{5/2}$
$U_{03} \times 10^{10}$	2.08(14)	2.29(14)	1.95(17)	2.05(17)	$\text{cm}^{-1} \text{u}^3$
$A_{00} \times 10^{-1}$	5.046090(88)	5.0642587(62)	5.065030(11)	5.064254(14)	$\text{cm}^{-1}$
$\Delta_{\text{A}_{00}}^{\text{Ti}} \times 10^{-2}$	3.286(15)	—	—	—	
$A_{10} \times 10^3$	5.025(45)	4.245(42)	6.77(73)	4.93(84)	$\text{cm}^{-1} \text{u}^{1/2}$
$A_{20} \times 10^3$	-10.399(53)	-10.421(54)	-10.61(51)	-10.88(53)	$\text{cm}^{-1} \text{u}$
$A_{01} \times 10^4$	-3.12190(99)	1.895(24)	-1.797(10)	1.722(56)	$\text{cm}^{-1} \text{u}$
$\Delta_{\text{A}_{01}}^{\text{Ti}} \times 10^{-4}$	—	—	6.429(85)	—	
$A_{11} \times 10^5$	-3.958(63)	—	-4.25(22)	7.3(28)	$\text{cm}^{-1} \text{u}^{3/2}$
$\gamma_{01} \times 10^2$	—	9.326(45)	—	9.00(10)	$\text{cm}^{-1} \text{u}$

**Table 2** continued on next page

**Table 2** (*continued*)

Parameter	This work		Ref. <sup>a</sup>		Units
	Fit A	Fit B	Fit A	Fit B	
$\hat{O}_{k,l}$					
$\gamma_{11} \times 10^2$	–	0.952(12)	–	2.36(52)	$\text{cm}^{-1} \text{u}^{3/2}$
$\gamma_{02} \times 10^7$	–	5.10(191)	–	–	$\text{cm}^{-1} \text{u}^2$
$\lambda_{00}$	1.749446(62)	1.745255(65)	1.74974(16)	1.74584(18)	$\text{cm}^{-1}$
$\lambda_{10} \times 10^2$	-1.5066(29)	-1.5454(22)	-1.81(11)	-2.00(12)	$\text{cm}^{-1} \text{u}^{1/2}$
$\lambda_{20} \times 10^3$	–	–	3.19(85)	3.13(85)	$\text{cm}^{-1} \text{u}$
$\lambda_{01} \times 10^6$	5.65(20)	-48.60(29)	6.64(15)	-47.76(44)	$\text{cm}^{-1} \text{u}$
$\lambda_{11} \times 10^8$	4.7(10)	–	–	–	$\text{cm}^{-1} \text{u}^{3/2}$
$a_{00} \times 10^3$	5.6198(21)	5.6136(22)	5.6220(45)	5.6133(46)	$\text{cm}^{-1} g_N^{-1}$
$\Delta a_{00} \times 10^3$	4.613(16)	4.647(16)	4.620(31)	4.684(31)	$\text{cm}^{-1} g_N^{-1} \text{u}^{1/2}$
$b_{00} \times 10^2$	2.7470(11)	2.7658(12)	2.7481(30)	2.7653(26)	$\text{cm}^{-1} g_N^{-1}$
$c_{00} \times 10^3$	-2.9640(87)	-3.1638(91)	-2.971(20)	-3.160(20)	$\text{cm}^{-1} g_N^{-1}$
$c_{01} \times 10^4$	1.239(17)	1.204(17)	1.257(37)	1.205(38)	$\text{cm}^{-1} g_N^{-1} \text{u}$
$eQq_{000} \times 10^3$	-6.03184(55)	-6.03246(56)	-6.0320(11)	-6.0322(11)	$\text{cm}^{-1} \text{b}^{-1}$

<sup>a</sup>Values taken from Breier et al. (2019)

## 5. MASS-INDEPENDANT DUNHAM-LIKE PARAMETERIZATION

The addition of new mid-IR ro-vibrational transitions confirm and improve the former mass-independent Dunham-like parameterization (Breier et al. 2019), see Table 2. This can be seen, when comparing the equilibrium bond length of  $^{48}\text{Ti}^{16}\text{O}$  ( $r_e^{48}$ ) with previous works, see Table 3. The here derived value of  $r_e^{48}=1.62033700(14)\text{\AA}$  is in perfect agreement with the single isotopologue study of Ram et al. (1999) ( $r_e^{48}=1.62033709(25)\text{\AA}$ ) and with the former multi-isotopologue study of Breier et al. (2019) ( $r_e^{48}=1.62033696(7)\text{\AA}$ ). The agreement with the previous works, is also reflected by the

**Table 3.** Comparison of bond length model values for TiO.

	Bond length (Å)	Ref.
$r_e^{48}$	1.62033709(25)	Ram et al. (1999)
	1.62033696(7)	Breier et al. (2019)
	1.62033700(14)	this work
$r_e^{\text{BO}}$	1.61999035(93) <sup>a</sup>	Breier et al. (2019)
	1.61998846(90)	this work

<sup>a</sup>Derived from parameter  $U_{01}$  of Fit B listed in Tab.11 (Breier et al. 2019)

Born-Oppenheimer corrected bond length of TiO  $r_e^{\text{BO}}$ , evaluated from the  $U_{01}$  parameter, see Table 3. The difference between the here derived  $r_e^{\text{BO}}$  and  $r_e^{48}$  is solely related to BO correction terms.

### 5.1. Born-Oppenheimer correction coefficients

With the present TiO parameterization (“Fit B”), three mass-dependent BO correction parameters, namely  $\Delta_{U_{01}}^{\text{Ti}}$ ,  $\Delta_{U_{01}}^{\text{O}}$  and  $\Delta_{U_{10}}^{\text{Ti}}$  are determined, see Table 4. By comparing the derived  $U_{01}$  correction values with those derived from theoretical calculations ( $\Delta_{U_{01}}^{\text{Ti}} = -4.9$  and  $\Delta_{U_{01}}^{\text{O}} = -6.7$ , Breier et al. (2019)), an almost constant shift of 3 to 3.4 is observed. Besides this difference in absolute values, the experimental results follow the same trend as the calculated  $\Delta_{U_{01}}^{\text{Ti}}$  and  $\Delta_{U_{01}}^{\text{O}}$  values, i.e., in both cases the contribution to the mass shift of rotational energy levels is stronger for oxygen than for titanium. The same trend is also observed in the case of ZrO and HfO (Table 4). Furthermore, the vibrational mass correction value of  $U_{10}$  for titanium is derived here in the same order as expected from CO and SiO, see Table 4.

By using the Born-Oppenheimer mass correction values  $\Delta_{U_{10}}^{\text{A}}$  and  $\Delta_{U_{01}}^{\text{A}}$  for an atom A, Ogilvie (1989) derived an empirical relation to estimate the mass correction value  $\Delta_{U_{02}}^{\text{A}}$  for the first order centrifugal distortion term  $U_{02}$ . In case of titanium it is as follows

$$\Delta_{U_{02}}^{\text{Ti}} \approx 3\Delta_{U_{01}}^{\text{Ti}} - 2\Delta_{U_{10}}^{\text{Ti}}, \quad (2)$$

**Table 4.** Comparison of Born-Oppenheimer correction values for diatomic molecules of the form AB, i.e., TiO, CO, SiO, ZrO and HfO.

	This work	Ref. <sup>a</sup>	Ref. <sup>b</sup>	Ref. <sup>c</sup>	Ref. <sup>d</sup>
	TiO	CO	SiO	ZrO	HfO
$\Delta_{U_{10}}^A$	0.114(31)	0.69547(7)	0.567(37)	–	–
$\Delta_{U_{10}}^B$	–	-0.16886(7)	–	–	–
$\Delta_{U_{01}}^A$	-8.314(16)	-2.0567(2)	-1.2976(44)	-4.872(39)	-3.40(57)
$\Delta_{U_{01}}^B$	-9.769(31)	-2.1047(2)	-2.0507(16)	-6.1888(25)	-5.656(23)

<sup>a</sup>Values taken from [Velichko et al. \(2012\)](#)

<sup>b</sup>Values taken from [Müller et al. \(2013\)](#)

<sup>c</sup>Values taken from [Beaton & Gerry \(1999\)](#)

<sup>d</sup>Values taken from [Lesarri et al. \(2002\)](#)

yielding  $\Delta_{02}^{\text{Ti}} = -25.2(1)$ . By applying the Kratzer-Pekeris relation ([Kratzer 1920](#); [Pekeris 1934](#)) to  $U_{01}$  and  $U_{10}$ , the mass independent first order centrifugal distortion term  $U_{02}^{\text{BO}} = 8.67932(3) \times 10^{-5} \text{ cm}^{-1}\text{u}^{-2}$  is calculated according to:

$$U_{02}^{\text{BO}} = \frac{4U_{01}^3}{U_{10}^2}. \quad (3)$$

In contrast to  $U_{02}$ , the BO correction is considered for  $U_{02}^{\text{BO}}$ , and consequently their combination with  $\Delta_{02}^{\text{Ti}}$  allows to calculate the corresponding oxygen Born-Oppenheimer correction value  $\Delta_{U_{02}}^O = -15(1)$  according to Equation 1.

### 5.2. Spin-rotation coupling constant

For a diatomic molecule in a multiplet state ( $\Lambda > 0$ ), the contribution of the spin-rotation interaction and the centrifugal correction of the spin-orbit coupling to the energy levels are only distinguishable in a multi-isotopic fitting procedure ([Müller et al. 2013](#)). In this work, the spin-rotation coupling constant  $\gamma$  for the  $X^3\Delta$  ground-state of TiO was determined for the first time. [Brown & Watson \(1977\)](#) have shown that the spin-rotation interaction  $\gamma \hat{\mathbf{N}} \cdot \hat{\mathbf{S}}$  consists of two contributions  $\gamma^{(1)}$  and  $\gamma^{(2)}$ , with  $\gamma^{(1)}$  describing the first-order dipole-dipole interaction contribution of electronic spin and the

rotating charges and  $\gamma^{(2)}$  introduces the second-order spin-orbit interaction contribution (Brown & Watson (1977)). The term  $\gamma^{(2)}$  dominates in case of molecules with a large spin-orbit interaction. According to Lefebvre-Brion & Field (1986) and assuming a microscopic description of the spin-orbital operator in a single configuration representation for the electronic states, the spin-rotation coupling constant  $\gamma$  can be estimated to be

$$\gamma = \gamma^{(1)} + \gamma^{(2)} \approx 2 \frac{\bar{A} \cdot \bar{B}}{E_{E^3\Pi} - E_{X^3\Delta}} = \gamma^{E-X}. \quad (4)$$

If we consider only contributions from the two lowest lying triplet configuration state  $X^3\Delta$  and  $E^3\Pi$  ( $E_{E^3\Pi} - E_{X^3\Delta} = 11826.9548(5) \text{ cm}^{-1}$ ) of TiO (Kobayashi et al. (2002)) and assume an average spin-orbital contribution of both states of  $\bar{A} = 94.0513(5) \text{ cm}^{-1}$  as well as an average rotational constant of  $\bar{B} = 0.524442(4) \text{ cm}^{-1}$ , we obtain a spin-rotation coupling constant of  $\gamma^{E-X} = 250.058(2) \text{ MHz}$  from Equation 4. This value is in fairly good agreement with our experimental value of  $\gamma = 236.5(11) \text{ MHz}$  suggesting that the strongest contribution of the spin-rotation coupling occurs from the interaction between the states of  $E^3\Pi$  and  $X^3\Delta$ .

### 5.3. Vibrational Transition Moments

Finally, the vibrational transition moments for the observed vibrational transitions  $\nu_{i \leftarrow i-1}$  are calculated. We have utilized the Dunham-like parameterization of TiO to generate the electronic ground-state potential of TiO using the Rydberg-Klein-Rees description (Rydberg 1932, 1933; Klein 1932; Rees 1947). The potential constants are generated with the RKR1 program from Le Roy (2017). The potential is combined with diagonal elements of the dipole moment curve of the  $X^3\Delta$  electronic ground-state taken from McKemmish et al. (2019) to determine the vibrational transition moments with the DUO software (Yurchenko et al. 2016). The results are listed in Table 1 and are in excellent agreement with the values reported in the literature. Furthermore, the calculated vibrational transition moments allow to reproduce the line intensities measured in our experiments very well, as depicted in Figure 1.

## 6. CONCLUSION

In this work, we report on 1034 ro-vibrational transitions of TiO around  $1000\text{ cm}^{-1}$ . Accurate experimental frequency positions with an uncertainty of better than  $10^{-3}\text{ cm}^{-1}$  are provided in the supplementary material, see Tables 5 to 12. We have identified the fundamental bands of the stable isotopologues  $^{46-50}\text{TiO}$ , as well as the three lowest lying vibrational hotbands of the main isotopologue  $^{48}\text{TiO}$ . Our data can be used to guide the astronomical search for TiO at infrared frequencies. The tentative detection of TiO towards the S-type star NP Aurigae using low resolution spectra at  $1000\text{ cm}^{-1}$  from the *Spitzer Space Telescope* (Smolders et al. 2012) could be reexamined, using telescopes with high spectral resolution instruments such as EXES or TEXES ( $R \sim 100,000$ ) to unambiguously verify this assignment.

The previous mass-independent Dunham-like parameterization of TiO (Breier et al. 2019) is improved by including experimental mid-IR data of the present study. Our analysis yields a reliable parameterization of the spin-rotation coupling constant  $\gamma$  with strong contributions occurring between the states  $E^3\Pi$  and  $X^3\Delta$ . Furthermore, additional Born-Oppenheimer correction coefficients  $\Delta_{U_{01}}^{\text{Ti}}$ ,  $\Delta_{U_{02}}^{\text{Ti}}$  and  $\Delta_{U_{02}}^{\text{O}}$  have been determined. This enables accurate predictions of highly excited ro-vibrational states of rare TiO isotopologues, such as  $^{44}\text{TiO}$ , within the uncertainty accuracy of the main isotopologue. In addition, the vibrational transition moments are calculated from the Dunham-like parameterization using a RKR potential description as input for the DUO software.

## ACKNOWLEDGMENT

This paper is dedicated to the 60<sup>th</sup> birthday of Stephan Schlemmer from the Universität zu Köln. His friendship and inspiring work in the field of molecular spectroscopy benefited us all. The authors gratefully acknowledge many fruitful discussions, support and advices from Stephan on various occasions. This work is supported by the Deutsche Forschungsgemeinschaft (DFG, German Research Foundation) project number 328961117 - SFB 1319 ELCH and project number 326572190 - FU 715/2-1.

## SUPPLEMENTARY MATERIALS

The supplementary materials contain lists of the observed infrared transitions for  $^{46-50}\text{TiO}$  and the molecular parameters for the electronic states  $A^3\Phi$  and  $B^3\Pi$ .

## REFERENCES

- Amiot, C., Azaroual, E. M., Luc, P., & Vetter, R. 1995, J. Chem. Phys., 102, 4375, doi: [10.1063/1.469486](https://doi.org/10.1063/1.469486)
- Amiot, C., Cheikh, M., Luc, P., & Vetter, R. 1996, J. Mol. Spectrosc., 179, 159, doi: [10.1006/jmsp.1996.0194](https://doi.org/10.1006/jmsp.1996.0194)
- Austin, S. M., West, C., & Heger, A. 2017, Astrophys. J. Lett., 839, L9, doi: [10.3847/2041-8213/aa68e7](https://doi.org/10.3847/2041-8213/aa68e7)
- Barnbaum, C., Omont, A., & Morris, M. 1996, Astron. Astrophys., 310, 259. <http://adsabs.harvard.edu/abs/1996A%26A...310..259B>
- Beaton, S. A., & Gerry, M. C. L. 1999, J. Chem. Phys., 110, 10715, doi: [10.1063/1.479014](https://doi.org/10.1063/1.479014)
- Breier, A. A., Waßmuth, B., Büchling, T., et al. 2018, J. Mol. Spectrosc., 350, 43, doi: [10.1016/j.jms.2018.06.001](https://doi.org/10.1016/j.jms.2018.06.001)
- Breier, A. A., Waßmuth, B., Fuchs, G. W., Gauss, J., & Giesen, T. F. 2019, J. Mol. Spectrosc., 355, 46, doi: [10.1016/j.jms.2018.11.006](https://doi.org/10.1016/j.jms.2018.11.006)
- Brown, J. M., & Watson, J. K. G. 1977, J. Mol. Spectrosc., 65, 65, doi: [10.1016/0022-2852\(77\)90358-7](https://doi.org/10.1016/0022-2852(77)90358-7)
- Chavez, J., & Lambert, D. L. 2009, Astrophys. J., 699, 1906, doi: [10.1088/0004-637X/699/2/1906](https://doi.org/10.1088/0004-637X/699/2/1906)
- Danilovich, T., Gottlieb, C. A., Decin, L., et al. accepted 2020, Astrophys. J., doi: <https://arxiv.org/pdf/2010.06485.pdf>
- De Laeter, J. R., Böhlke, J. K., De Bièvre, P., et al. 2003, Pure Appl. Chem., 75, 683, doi: [10.1351/pac200375060683](https://doi.org/10.1351/pac200375060683)
- Dunham, J. L. 1932a, Phys. Rev., 41, 713, doi: [10.1103/PhysRev.41.713](https://doi.org/10.1103/PhysRev.41.713)
- . 1932b, Phys. Rev., 41, 721, doi: [10.1103/PhysRev.41.721](https://doi.org/10.1103/PhysRev.41.721)
- Evans, T. M., Sing, D. K., Wakeford, H. R., et al. 2016, Astrophys. J. Lett., 822, L4, doi: [10.3847/2041-8205/822/1/L4](https://doi.org/10.3847/2041-8205/822/1/L4)
- Fletcher, D. A., Scurlock, C. T., Jung, K. Y., & Steimle, T. C. 1993, J. Chem. Phys., 99, 4288, doi: [10.1063/1.466082](https://doi.org/10.1063/1.466082)
- Fowler, A. 1904, Proc. R. Soc. London, 73, 219. <http://www.jstor.org/stable/116773>
- Herriott, D., Kogelnik, H., & Kompfner, R. 1964, Appl. Opt., 3, 523, doi: [10.1364/AO.3.000523](https://doi.org/10.1364/AO.3.000523)
- Huitson, C. M., Sing, D. K., Pont, F., et al. 2013, Mon. Notices Royal Astron. Soc., 434, 3252, doi: [10.1093/mnras/stt1243](https://doi.org/10.1093/mnras/stt1243)
- Kamiński, T., Schmidt, M., & Tylenda, R. 2010, Astron. Astrophys., 522, A75, doi: [10.1051/0004-6361/201014406](https://doi.org/10.1051/0004-6361/201014406)

- Kamiński, T., Gottlieb, C. A., Menten, K. M., et al. 2013, *Astron. Astrophys.*, 551, A113, doi: [10.1051/0004-6361/201220290](https://doi.org/10.1051/0004-6361/201220290)
- Kamiński, T., Müller, H. S. P., Schmidt, M. R., et al. 2017, *Astron. Astrophys.*, 599, A59, doi: [10.1051/0004-6361/201629838](https://doi.org/10.1051/0004-6361/201629838)
- Kania, P., Giesen, T. F., Müller, H. S. P., Schlemmer, S., & Brünken, S. 2008, in 2008 33rd International Conference on Infrared, Millimeter and Terahertz Waves, 1–2, doi: [10.1109/ICIMW.2008.4665795](https://doi.org/10.1109/ICIMW.2008.4665795)
- Klein, O. 1932, *Zeits. f. Physik*, 76, 226, doi: [10.1007/BF01341814](https://doi.org/10.1007/BF01341814)
- Kobayashi, K., Hall, G. E., Muckerman, J. T., Sears, T. J., & Merer, A. J. 2002, *J. Mol. Spectrosc.*, 212, 133, doi: [10.1006/jmsp.2002.8543](https://doi.org/10.1006/jmsp.2002.8543)
- Kratzer, A. 1920, *Zeits. f. Physik*, 3, 289, doi: [10.1007/BF01327754](https://doi.org/10.1007/BF01327754)
- Le Roy, R. J. 2017, *J. Quant. Spectrosc. Radiat. Transfer*, 186, 158, doi: [10.1016/j.jqsrt.2016.03.030](https://doi.org/10.1016/j.jqsrt.2016.03.030)
- Lefebvre-Brion, H., & Field, R. W. 1986, Perturbations in the Spectra of Diatomic Molecules (Academic, Orlando)
- Lesarri, A., Suenram, R. D., & Brugh, D. 2002, *J. Chem. Phys.*, 117, 9651, doi: [10.1063/1.1516797](https://doi.org/10.1063/1.1516797)
- Lincowski, A. P., Halfen, D. T., & Ziurys, L. M. 2016, *Astrophys. J.*, 833, 9, doi: [10.3847/0004-637X/833/1/9](https://doi.org/10.3847/0004-637X/833/1/9)
- Lowater, F. 1929, *Natur*, 123, 644, doi: [10.1038/123644b0](https://doi.org/10.1038/123644b0)
- McKemmish, L. K., Masseron, T., Hoeijmakers, H. J., et al. 2019, *Mon. Notices Royal Astron. Soc.*, 488, 2836, doi: [10.1093/mnras/stz1818](https://doi.org/10.1093/mnras/stz1818)
- McKemmish, L. K., Masseron, T., Sheppard, S., et al. 2017, *Astrophys. J. Suppl. Ser.*, 228, 15, doi: [10.3847/1538-4365/228/2/15](https://doi.org/10.3847/1538-4365/228/2/15)
- Merrill, P. W., Deutsch, A. J., & Keenan, P. C. 1962, *Astrophys. J.*, 1, 21, doi: [10.1086/147348](https://doi.org/10.1086/147348)
- Morgan, W. W., & Keenan, P. C. 1973, *Annu. Rev. Astron. Astrophys.*, 11, 29, doi: [10.1146/annurev.aa.11.090173.000333](https://doi.org/10.1146/annurev.aa.11.090173.000333)
- Müller, H. S. P., Kobayashi, K., Takahashi, K., Tomaru, K., & Matsushima, F. 2015, *J. Mol. Spectrosc.*, 310, 92, doi: [10.1016/j.jms.2014.12.002](https://doi.org/10.1016/j.jms.2014.12.002)
- Müller, H. S. P., Spezzano, S., Bizzocchi, L., et al. 2013, *J. Phys. Chem. A*, 117, 13843, doi: [10.1021/jp408391f](https://doi.org/10.1021/jp408391f)
- Namiki, K.-i. C., & Ito, H. 2002, *J. Mol. Spectrosc.*, 214, 188, doi: [10.1006/jmsp.2002.8586](https://doi.org/10.1006/jmsp.2002.8586)
- Namiki, K.-i. C., Ito, H., & Davis, S. P. 2003, *J. Mol. Spectrosc.*, 217, 173, doi: [10.1016/S0022-2852\(02\)00027-9](https://doi.org/10.1016/S0022-2852(02)00027-9)
- Namiki, K.-i. C., Saitoh, H., & Ito, H. 2004, *J. Mol. Spectrosc.*, 226, 87, doi: [10.1016/j.jms.2004.03.016](https://doi.org/10.1016/j.jms.2004.03.016)
- Ogilvie, J. F. 1989, *Spectrosc. Lett.*, 22, 477, doi: [10.1080/00387018908053897](https://doi.org/10.1080/00387018908053897)
- Pavlenko, Y. V., Yurchenko, S. N., McKemmish, L. K., & Tennyson, J. 2020, *Astron. Astrophys.*, 642, A77, doi: [10.1051/0004-6361/202037863](https://doi.org/10.1051/0004-6361/202037863)

- Pekeris, C. L. 1934, Phys. Rev., 45, 98,  
doi: [10.1103/PhysRev.45.98](https://doi.org/10.1103/PhysRev.45.98)
- Phillips, J. G. 1950, Astrophys. J., 111, 314,  
doi: [10.1086/145266](https://doi.org/10.1086/145266)
- . 1951, Astrophys. J., 114, 152,  
doi: [10.1086/145460](https://doi.org/10.1086/145460)
- . 1969, Astrophys. J., 157, 449,  
doi: [10.1086/150079](https://doi.org/10.1086/150079)
- Piette, A. A. A., Madhusudhan, N., McKemmish, L. K., et al. 2020, Mon. Notices Royal Astron. Soc., 496, 3870, doi: [10.1093/mnras/staa1592](https://doi.org/10.1093/mnras/staa1592)
- Ram, R. S., Bernath, P. F., Dulick, M., & Wallace, L. 1999, Astrophys. J. Suppl. Ser., 122, 331, doi: [10.1086/313212](https://doi.org/10.1086/313212)
- Ram, R. S., Bernath, P. F., & Wallace, L. 1996, Astrophys. J. Suppl. Ser., 107, 443,  
doi: [10.1086/192370](https://doi.org/10.1086/192370)
- Rees, A. L. G. 1947, Proc. Phys. Soc. (Lond), 59, 998, doi: [10.1088/0959-5309/59/6/310](https://doi.org/10.1088/0959-5309/59/6/310)
- Reid, M. J., & Goldston, J. E. 2002, Astrophys. J., 568, 931, doi: [10.1086/338947](https://doi.org/10.1086/338947)
- Rydberg, R. 1932, Zeits. f. Physik, 73, 376,  
doi: [10.1007/BF01341146](https://doi.org/10.1007/BF01341146)
- . 1933, Zeits. f. Physik, 80, 514,  
doi: [10.1007/BF02057312](https://doi.org/10.1007/BF02057312)
- Siegert, T., Diehl, R., Krause, M. G. H., & Greiner, J. 2015, Astron. Astrophys., 579, A124,  
doi: [10.1051/0004-6361/201525877](https://doi.org/10.1051/0004-6361/201525877)
- Sing, D. K., Lecavelier des Etangs, A., Fortney, J. J., et al. 2013, Mon. Notices Royal Astron. Soc., 436, 2956, doi: [10.1093/mnras/stt1782](https://doi.org/10.1093/mnras/stt1782)
- Smolders, K., Verhoelst, T., Neyskens, P., et al. 2012, Astron. Astrophys., 543, L2,  
doi: [10.1051/0004-6361/201219520](https://doi.org/10.1051/0004-6361/201219520)
- Tennyson, J., Yurchenko, S. N., Al-Refaie, A. F., et al. 2016, J. Mol. Spectrosc., 327, 73,  
doi: [10.1016/j.jms.2016.05.002](https://doi.org/10.1016/j.jms.2016.05.002)
- Tsygankov, S. S., Krivonos, R. A., Lutovinov, A. A., et al. 2016, Mon. Not. R. Astron. Soc., 458, 3411, doi: [10.1093/mnras/stw549](https://doi.org/10.1093/mnras/stw549)
- Velichko, T. I., Mikhailenko, S. N., & Tashkun, S. A. 2012, J. Quant. Spectrosc. Radiat. Transfer, 113, 1643,  
doi: [10.1016/j.jqsrt.2012.04.014](https://doi.org/10.1016/j.jqsrt.2012.04.014)
- Wang, M., Audi, G., Kondev, F. G., et al. 2017, Chin. Phys. C, 41, 030003,  
doi: [10.1088/1674-1137/41/3/030003](https://doi.org/10.1088/1674-1137/41/3/030003)
- Watson, J. K. G. 2003, J. Mol. Spectrosc., 219, 326, doi: [10.1016/S0022-2852\(03\)00100-0](https://doi.org/10.1016/S0022-2852(03)00100-0)
- Western, C. M. 2017, J. Quant. Spectrosc. Radiat. Transfer, 186, 221,  
doi: [10.1016/j.jqsrt.2016.04.010](https://doi.org/10.1016/j.jqsrt.2016.04.010)
- Witsch, D., Lutter, V., Breier, A. A., et al. 2019, J. Phys. Chem. A, 123, 4168,  
doi: [10.1021/acs.jpca.9b01605](https://doi.org/10.1021/acs.jpca.9b01605)
- Xu, L.-H., Lees, R. M., Wang, P., et al. 2004, J. Mol. Spectrosc., 228, 453,  
doi: [10.1016/j.jms.2004.05.017](https://doi.org/10.1016/j.jms.2004.05.017)
- Yurchenko, S. N., Lodi, L., Tennyson, J., & Stolyarov, A. V. 2016, Comput. Phys. Commun., 202, 262,  
doi: [10.1016/j.cpc.2015.12.021](https://doi.org/10.1016/j.cpc.2015.12.021)

## APPENDIX

## A. SUPPLEMENTARY MATERIAL

**Table 5.** Observed transitions for  $^{48}\text{TiO}$ ,  $v = 1 \leftarrow 0$ . Experimental errors for line positions are better than  $1 \times 10^{-3} \text{ cm}^{-1}$ .

$J'$	$\Omega'$	$J''$	$\Omega''$	Frequency	Obs-Calc	$E_{\text{lower}}$	$J'$		$\Omega'$	$J''$	$\Omega''$	Frequency	Obs-Calc	$E_{\text{lower}}$
							cm $^{-1}$	$10^{-4} \text{ cm}^{-1}$						
25	3	24	3	971.264	1.1	954.0184	25	1	24	1	971.8669	4.76	748.4708	
24	2	23	2	972.7568	1.2	822.4359	23	3	22	3	973.7034	4.13	901.2496	
23	1	22	1	974.253	2.79	696.7772	22	3	21	3	974.9134	-4.19	876.4754	
22	2	21	2	975.1595	1.08	772.2968	22	1	21	1	975.4376	3.41	672.51	
21	3	20	3	976.119	1.24	852.7754	21	2	20	2	976.3521	0.68	748.8236	
21	1	20	1	976.6167	6.57	649.2964	20	3	19	3	977.3183	3.03	830.1499	
20	2	19	2	977.5393	3.34	726.4151	20	1	19	1	977.7897	5.84	627.1364	
19	2	18	2	978.7201	0.33	705.0716	18	3	17	3	979.6993	4.15	788.1239	
18	2	17	2	979.8953	-0.47	684.7934	18	1	17	1	980.1181	2.72	585.9782	
17	3	16	3	980.8808	3.42	768.7242	17	2	16	2	981.0645	-2.78	665.5808	
17	1	16	1	981.2736	1.88	566.9805	16	3	15	3	982.0568	6.2	750.4003	
16	2	15	2	982.2284	-0.61	647.434	16	1	15	1	982.4235	2.04	549.0372	
15	3	14	3	983.226	0.31	733.1527	15	2	14	2	983.3862	0.04	630.3534	
15	1	14	1	983.568	6.5	532.1485	14	3	13	3	984.3897	-0.15	716.9817	
14	2	13	2	984.5379	-1.95	614.3391	14	1	13	1	984.7058	1.5	516.3146	
13	3	12	3	985.5479	2.56	701.8874	13	2	12	2	985.684	-1.04	599.3914	
13	1	12	1	985.8377	-2.97	501.5357	12	3	11	3	986.6995	-0.01	687.8703	
12	2	11	2	986.824	-2.6	585.5105	12	1	11	1	986.9651	4.5	487.8118	
11	3	10	3	987.8461	6.38	674.9304	11	2	10	2	987.9587	3.12	572.6966	
11	1	10	1	988.0858	3.81	475.1431	10	3	9	3	988.9854	1.21	663.0681	

**Table 5** continued on next page

**Table 5.** (*continued*)

$J'$	$\Omega'$	$J''$	$\Omega''$	Frequency	Obs-Calc	$E_{\text{lower}}$	$J'$	$\Omega'$	$J''$	$\Omega''$	Frequency	Obs-Calc	$E_{\text{lower}}$
				$\text{cm}^{-1}$	$10^{-4} \text{ cm}^{-1}$	K					$\text{cm}^{-1}$	$10^{-4} \text{ cm}^{-1}$	K
10	2	9	2	989.0861	-5.71	560.9499	10	1	9	1	989.2003	0.0	463.5298
9	3	8	3	990.1195	3.48	652.2835	9	2	8	2	990.2087	-3.86	550.2705
9	1	8	1	990.3095	1.56	452.9718	8	3	7	3	991.248	9.56	642.5769
8	2	7	2	991.3252	-1.66	540.6587	8	1	7	1	991.4121	-4.28	443.4694
7	3	6	3	992.3694	6.53	633.9483	7	2	6	2	992.4361	2.9	532.1144
7	1	6	1	992.5104	6.0	435.0226	6	3	5	3	993.4851	6.74	626.398
6	2	5	2	993.5402	-0.01	524.638	6	1	5	1	993.6015	3.17	427.6315
5	3	4	3	994.5948	7.83	619.9261	5	2	4	2	994.6389	2.3	518.2294
5	1	4	1	994.6874	6.33	421.2961	4	3	3	3	995.6978	3.7	614.5326
4	2	3	2	995.7311	0.13	512.8887	4	1	3	1	995.7668	3.9	416.0165
3	2	2	2	996.8176	1.46	508.6161	3	1	2	1	996.8409	7.29	411.7928
2	1	1	1	997.9085	5.14	408.625	21	3	21	3	998.6149	10.54	852.7754
20	3	20	3	998.7449	5.83	830.1499	19	3	19	3	998.8694	7.57	808.5993
18	3	18	3	998.9869	1.09	788.1239	18	2	18	2	998.9989	5.81	684.7934
18	1	18	1	999.0086	2.56	585.9782	17	3	17	3	999.0994	7.4	768.7242
17	2	17	2	999.1084	4.0	665.5808	17	1	17	1	999.1157	1.1	566.9805
16	3	16	3	999.2049	5.64	750.4003	16	2	16	2	999.2116	0.58	647.434
16	1	16	1	999.2175	7.41	549.0372	15	3	15	3	999.3039	1.87	733.1527
15	2	15	2	999.3093	1.55	630.3534	15	1	15	1	999.312	0.0	532.1485
14	3	14	3	999.3973	3.18	716.9817	14	2	14	2	999.4008	2.67	614.3391
14	1	14	1	999.4013	0.5	516.3146	13	1	13	1	999.485	4.38	501.5357
13	2	13	2	999.485	-7.96	599.3914	13	3	13	3	999.485	10.24	701.8874
12	1	12	1	999.5618	-1.66	487.8118	12	2	12	2	999.565	-0.26	585.5105
12	3	12	3	999.565	2.12	687.8703	11	1	11	1	999.6333	-0.31	475.1431
11	2	11	2	999.6381	-0.77	572.6966	11	3	11	3	999.64	5.95	674.9304

**Table 5** continued on next page

**Table 5.** (*continued*)

$J'$	$\Omega'$	$J''$	$\Omega''$	Frequency	Obs-Calc	$E_{\text{lower}}$	$J'$	$\Omega'$	$J''$	$\Omega''$	Frequency	Obs-Calc	$E_{\text{lower}}$
				$\text{cm}^{-1}$	$10^{-4} \text{ cm}^{-1}$	K					$\text{cm}^{-1}$	$10^{-4} \text{ cm}^{-1}$	K
10	1	10	1	999.6992	4.29	463.5298	10	2	10	2	999.7048	-3.78	560.9499
10	3	10	3	999.7078	0.69	663.0681	9	1	9	1	999.7581	-0.78	452.9718
9	2	9	2	999.7659	-2.12	550.2705	9	3	9	3	999.7702	2.67	652.2835
8	1	8	1	999.8121	3.75	443.4694	8	2	8	2	999.8207	-1.7	540.6587
8	3	8	3	999.8264	5.66	642.5769	7	1	7	1	999.8598	4.55	435.0226
7	2	7	2	999.8699	3.05	532.1144	7	3	7	3	999.8763	7.82	633.9483
6	1	6	1	999.9013	3.97	427.6315	6	2	6	2	999.9124	1.56	524.638
6	3	6	3	999.9199	7.99	626.398	5	1	5	1	999.9368	1.93	421.2961
5	2	5	2	999.9488	-0.77	518.2294	5	3	5	3	999.9569	5.44	619.9261
4	1	4	1	999.9668	4.25	416.0165	4	2	4	2	999.9793	0.15	512.8887
4	3	4	3	999.9879	4.46	614.5326	3	1	3	1	999.9899	-2.44	411.7928
3	2	3	2	1000.0034	-2.74	508.6161	2	1	2	1	1000.0081	1.52	408.625
3	3	3	3	1000.0127	4.47	610.2177	1	1	1	1	1000.0215	16.7	406.5131
2	2	2	2	1000.0215	-4.25	505.4116	1	1	2	1	1002.12	1.6	406.5131
2	1	3	1	1003.1582	2.4	408.625	2	2	3	2	1003.2084	2.07	505.4116
3	1	4	1	1004.1906	5.64	411.7928	3	2	4	2	1004.252	0.61	508.6161
3	3	4	3	1004.3031	8.44	610.2177	4	1	5	1	1005.2166	3.75	416.0165
4	3	5	3	1005.3491	-7.1	614.5326	5	1	6	1	1006.2367	4.12	421.2961
5	2	6	2	1006.3208	-0.54	518.2294	5	3	6	3	1006.3916	6.12	619.9261
6	1	7	1	1007.2508	3.59	427.6315	6	2	7	2	1007.3461	0.03	524.638
6	3	7	3	1007.4263	4.76	626.398	7	1	8	1	1008.2592	6.22	435.0226
7	2	8	2	1008.365	-1.11	532.1144	7	3	8	3	1008.4551	6.9	633.9483
8	1	9	1	1009.261	3.74	443.4694	8	2	9	2	1009.3779	0.0	540.6587
8	3	9	3	1009.4772	6.22	642.5769	9	1	10	1	1010.257	3.58	452.9718
9	2	10	2	1010.3847	1.57	550.2705	9	3	10	3	1010.4931	8.24	652.2835

**Table 5** continued on next page

**Table 5.** (*continued*)

$J'$	$\Omega'$	$J''$	$\Omega''$	Frequency	Obs-Calc	$E_{\text{lower}}$	$J'$	$\Omega'$	$J''$	$\Omega''$	Frequency	Obs-Calc	$E_{\text{lower}}$
				$\text{cm}^{-1}$	$10^{-4} \text{ cm}^{-1}$	K					$\text{cm}^{-1}$	$10^{-4} \text{ cm}^{-1}$	K
10	1	11	1	1011.2468	0.84	463.5298	10	2	11	2	1011.3849	0.0	560.9499
10	3	11	3	1011.5021	3.85	663.0681	11	1	12	1	1012.2308	1.78	475.1431
11	2	12	2	1012.3779	-10.6	572.6966	11	3	12	3	1012.5049	2.1	674.9304
12	1	13	1	1013.2079	-5.04	487.8118	12	2	13	2	1013.3669	1.86	585.5105
12	3	13	3	1013.5016	4.45	687.8703	13	1	14	1	1014.1806	4.05	501.5357
13	2	14	2	1014.3481	-1.33	599.3914	13	3	14	3	1014.4924	12.15	701.8874
14	1	15	1	1015.1463	4.01	516.3146	14	2	15	2	1015.3234	0.55	614.3391
14	3	15	3	1015.4752	4.36	716.9817	15	1	16	1	1016.1058	3.52	532.1485
15	2	16	2	1016.2924	1.9	630.3534	15	3	16	3	1016.4521	2.28	733.1527
16	1	17	1	1017.0587	-1.17	549.0372	16	2	17	2	1017.2548	0.29	647.434
16	3	17	3	1017.4229	3.92	750.4003	17	1	18	1	1018.0069	7.67	566.9805
17	2	18	2	1018.2113	3.95	665.5808	17	3	18	3	1018.3865	0.15	768.7242
18	1	19	1	1018.9477	4.66	585.9782	18	2	19	2	1019.161	2.95	684.7934
18	3	19	3	1019.3444	3.45	788.1239	19	2	20	2	1020.1042	1.56	705.0716
19	3	20	3	1020.2954	4.35	808.5993	20	1	21	1	1020.8116	6.67	627.1364
20	2	21	2	1021.0415	4.24	726.4151	20	3	21	3	1021.2395	2.06	830.1499
21	1	22	1	1021.7335	-0.1	649.2964	21	2	22	2	1021.9715	-1.18	748.8236
21	3	22	3	1022.1773	2.35	852.7754	22	1	23	1	1022.6505	5.76	672.51
22	2	23	2	1022.8958	0.8	772.2968	22	3	23	3	1023.1078	-4.03	876.4754
23	1	24	1	1023.56	-0.21	696.7772	23	2	24	2	1023.8135	1.44	796.8344
23	3	24	3	1024.0331	3.61	901.2496	24	1	25	1	1024.4643	4.32	722.0975
24	2	25	2	1024.7244	-1.6	822.4359	24	3	25	3	1024.9509	2.76	927.0974
25	1	26	1	1025.3619	3.55	748.4708	25	2	26	2	1025.6296	3.85	849.1011
25	3	26	3	1025.8622	3.85	954.0184	26	1	27	1	1026.2533	3.89	775.8968
26	2	27	2	1026.5274	-0.48	876.8295	26	3	27	3	1026.7658	-4.3	982.0123

**Table 5** continued on next page

**Table 5.** (*continued*)

$J'$	$\Omega'$	$J''$	$\Omega''$	Frequency	Obs-Calc	$E_{\text{lower}}$	$J'$	$\Omega'$	$J''$	$\Omega''$	Frequency	Obs-Calc	$E_{\text{lower}}$
				$\text{cm}^{-1}$	$10^{-4} \text{ cm}^{-1}$	K					$\text{cm}^{-1}$	$10^{-4} \text{ cm}^{-1}$	K
27	1	28	1	1027.1382	2.57	804.3752	27	2	28	2	1027.4191	-0.02	905.6208
27	3	28	3	1027.6644	3.22	1011.0784	28	1	29	1	1028.0171	4.55	833.9058
28	2	29	2	1028.3042	-0.28	935.4746	28	3	29	3	1028.5553	1.74	1041.2165
29	1	30	1	1028.8895	3.92	864.4882	29	2	30	2	1029.1829	1.53	966.3904
29	3	30	3	1029.4395	0.18	1072.4258	30	1	31	1	1029.7559	7.55	896.1221
30	2	31	2	1030.0552	3.94	998.3678	30	3	31	3	1030.3169	-1.18	1104.706
31	1	32	1	1030.6152	3.56	928.8073	31	2	32	2	1030.9202	0.51	1031.4064
31	3	32	3	1031.1878	-0.85	1138.0565	32	1	33	1	1031.4688	5.84	962.5434
32	2	33	2	1031.7792	1.84	1065.5057							

**Table 6.** Observed transitions for  $^{48}\text{TiO}$ ,  $v = 2 \leftarrow 1$ . Experimental errors for line positions are better than  $1 \times 10^{-3} \text{ cm}^{-1}$ .

$J'$	$\Omega'$	$J''$	$\Omega''$	Frequency	Obs-Calc	$E_{\text{lower}}$	$J'$	$\Omega'$	$J''$	$\Omega''$	Frequency	Obs-Calc	$E_{\text{lower}}$
				$\text{cm}^{-1}$	$10^{-4} \text{ cm}^{-1}$	K					$\text{cm}^{-1}$	$10^{-4} \text{ cm}^{-1}$	K
17	3	16	3	971.8212	4.61	1767.8228	17	2	16	2	972.0063	3.94	1664.6888
17	1	16	1	972.216	7.99	1566.096	16	2	15	2	973.1647	6.6	1646.6456
16	1	15	1	973.3607	9.54	1548.2539	15	3	14	3	974.1554	4.42	1732.4565
15	2	14	2	974.3167	4.42	1629.6625	14	3	13	3	975.313	-0.26	1716.3786
14	2	13	2	975.4643	17.63	1613.7396	14	1	13	1	975.6325	13.79	1515.7159
13	2	12	2	976.6038	8.18	1598.8772	13	1	12	1	976.7589	8.28	1501.0202
12	3	11	3	977.612	6.72	1687.435	12	2	11	2	977.7382	7.96	1585.0755
12	1	11	1	977.8802	10.38	1487.3737	11	3	10	3	978.7517	2.07	1674.5698
11	2	10	2	978.8665	6.16	1572.3347	10	3	9	3	979.8855	0.08	1662.7758
10	2	9	2	979.9889	4.71	1560.655	10	1	9	1	980.1046	9.57	1463.2285

**Table 6** *continued on next page*

**Table 6.** (*continued*)

$J'$	$\Omega'$	$J''$	$\Omega''$	Frequency	Obs-Calc	$E_{\text{lower}}$	$J'$	$\Omega'$	$J''$	$\Omega''$	Frequency	Obs-Calc	$E_{\text{lower}}$
				$\text{cm}^{-1}$	$10^{-4} \text{ cm}^{-1}$	K					$\text{cm}^{-1}$	$10^{-4} \text{ cm}^{-1}$	K
9	3	8	3	981.0131	-3.98	1652.0534	9	2	8	2	981.1051	0.2	1550.0366
9	1	8	1	981.2081	10.73	1452.73	8	3	7	3	982.1354	0.05	1642.4027
8	2	7	2	982.2161	5.17	1540.4796	8	1	7	1	982.3057	11.16	1443.2811
7	3	6	3	983.2507	-4.49	1633.8239	7	2	6	2	983.3204	2.57	1531.9841
7	1	6	1	983.3973	11.3	1434.8819	6	3	5	3	984.3605	-3.85	1626.3171
6	2	5	2	984.4186	-0.97	1524.5502	6	1	5	1	984.4828	9.68	1427.5324
5	3	4	3	985.4644	-0.39	1619.8824	5	2	4	2	985.5117	4.29	1518.1782
5	1	4	1	985.5624	7.98	1421.2327	4	3	3	3	986.5646	28.28	1614.52
4	2	3	2	986.5973	-3.91	1512.868	4	1	3	1	986.6358	3.47	1415.9829
3	2	2	2	987.6782	1.47	1508.6198	3	1	2	1	987.7039	5.82	1411.7829
2	1	1	1	988.7658	5.18	1408.6329	15	3	15	3	990.139	0.46	1732.4565
14	3	14	3	990.2322	-6.08	1716.3786	13	3	13	3	990.3192	-11.39	1701.3714
12	3	12	3	990.4013	-3.03	1687.435	12	1	12	1	990.4054	8.6	1487.3737
12	2	12	2	990.4054	8.03	1585.0755	11	2	11	2	990.4771	-11.37	1572.3347
10	1	10	1	990.5407	-15.72	1463.2285	10	3	10	3	990.5456	2.26	1662.7758
10	2	10	2	990.5456	0.08	1560.655	9	1	9	1	990.6027	6.52	1452.73
9	2	9	2	990.6074	4.45	1550.0366	9	3	9	3	990.6082	2.2	1652.0534
8	1	8	1	990.6569	9.98	1443.2811	8	2	8	2	990.6629	8.3	1540.4796
8	3	8	3	990.6644	1.74	1642.4027	7	1	7	1	990.7048	9.7	1434.8819
7	2	7	2	990.7115	4.25	1531.9841	7	3	7	3	990.714	-1.86	1633.8239
6	1	6	1	990.7462	5.71	1427.5324	6	2	6	2	990.7535	-4.56	1524.5502
6	3	6	3	990.7576	-3.55	1626.3171	5	1	5	1	990.7819	3.67	1421.2327
5	2	5	2	990.7909	0.93	1518.1782	5	3	5	3	990.7966	11.17	1619.8824
4	1	4	1	990.812	5.25	1415.9829	4	2	4	2	990.8213	-1.27	1512.868
4	3	4	3	990.8267	-1.21	1614.52	3	1	3	1	990.8364	9.61	1411.7829

**Table 6** continued on next page

**Table 6.** (*continued*)

$J'$	$\Omega'$	$J''$	$\Omega''$	Frequency	Obs-Calc	$E_{\text{lower}}$	$J'$	$\Omega'$	$J''$	$\Omega''$	Frequency	Obs-Calc	$E_{\text{lower}}$
				$\text{cm}^{-1}$	$10^{-4} \text{ cm}^{-1}$	K					$\text{cm}^{-1}$	$10^{-4} \text{ cm}^{-1}$	K
3	2	3	2	990.8458	-1.5	1508.6198	2	2	2	2	990.8643	-0.13	1505.4335
1	1	1	1	990.8655	1.49	1406.5329	1	1	2	1	992.9544	10.01	1406.5329
2	1	3	1	993.9865	10.96	1408.6329	2	2	3	2	994.0315	-6.4	1505.4335
3	1	4	1	995.0123	8.61	1411.7829	3	2	4	2	995.0701	4.04	1508.6198
3	3	4	3	995.1179	10.77	1610.23	4	1	5	1	996.0323	9.04	1415.9829
4	2	5	2	996.101	0.88	1512.868	4	3	5	3	996.158	0.59	1614.52
5	1	6	1	997.0462	8.25	1421.2327	5	2	6	2	997.1264	3.92	1518.1782
5	3	6	3	997.1926	-0.42	1619.8824	6	1	7	1	998.0544	10.48	1427.5324
6	2	7	2	998.1452	2.21	1524.5502	6	3	7	3	998.2211	0.81	1626.3171
7	1	8	1	999.0564	12.28	1434.8819	7	2	8	2	999.1582	6.2	1531.9841
7	3	8	3	999.2428	-2.83	1633.8239	8	1	9	1	1000.0518	8.17	1443.2811
8	2	9	2	1000.1648	8.37	1540.4796	8	3	9	3	1000.2586	-0.65	1642.4027
9	1	10	1	1001.0417	9.99	1452.73	9	2	10	2	1001.1648	6.96	1550.0366
9	3	10	3	1001.2682	3.92	1652.0534	10	1	11	1	1002.0251	7.12	1463.2285
10	2	11	2	1002.1583	3.57	1560.655	10	3	11	3	1002.2706	0.56	1662.7758
11	1	12	1	1003.0028	9.0	1474.7764	11	2	12	2	1003.1458	3.34	1572.3347
11	3	12	3	1003.2669	0.66	1674.5698	12	1	13	1	1003.974	7.08	1487.3737
12	2	13	2	1004.1273	6.17	1585.0755	12	3	13	3	1004.2565	-1.4	1687.435
13	1	14	1	1004.9396	10.41	1501.0202	13	2	14	2	1005.1022	6.98	1598.8772
13	3	14	3	1005.2397	-2.9	1701.3714	14	1	15	1	1005.8986	8.9	1515.7159
14	2	15	2	1006.0709	8.4	1613.7396	14	3	15	3	1006.2169	0.62	1716.3786
15	1	16	1	1006.8522	14.9	1531.4605	15	2	16	2	1007.0328	6.06	1629.6625
15	3	16	3	1007.1869	-2.01	1732.4565	16	1	17	1	1007.7987	11.61	1548.2539
16	2	17	2	1007.9888	7.75	1646.6456	16	3	17	3	1008.151	1.98	1749.6046
17	1	18	1	1008.7393	11.09	1566.096	17	3	18	3	1009.1083	3.69	1767.8228

**Table 6** continued on next page

**Table 6.** (*continued*)

$J'$	$\Omega'$	$J''$	$\Omega''$	Frequency	Obs-Calc	$E_{\text{lower}}$	$J'$	$\Omega'$	$J''$	$\Omega''$	Frequency	Obs-Calc	$E_{\text{lower}}$
				$\text{cm}^{-1}$	$10^{-4} \text{ cm}^{-1}$	K					$\text{cm}^{-1}$	$10^{-4} \text{ cm}^{-1}$	K
18	1	19	1	1009.6739	12.07	1584.9866	18	2	19	2	1009.8809	5.05	1683.7917
18	3	19	3	1010.0582	-3.22	1787.1107	19	1	20	1	1010.6018	8.79	1604.9255
19	2	20	2	1010.8171	1.57	1703.9541	19	3	20	3	1011.002	-5.14	1807.468
20	1	21	1	1011.5237	7.86	1625.9124	20	2	21	2	1011.7478	7.57	1725.1757
20	3	21	3	1011.9397	-1.72	1828.8943	21	1	22	1	1012.439	2.43	1647.9473
21	2	22	2	1012.6717	10.94	1747.4562	21	3	22	3	1012.8705	-0.5	1851.3893
22	1	23	1	1013.3494	11.98	1671.0299	22	2	23	2	1013.5884	6.19	1770.7952
22	3	23	3	1013.7946	-0.25	1874.9525	23	1	24	1	1014.2522	6.5	1695.1599
23	2	24	2	1014.4996	10.99	1795.1925	23	3	24	3	1014.7113	-6.97	1899.5837
24	1	25	1	1015.1496	11.57	1720.3372	24	2	25	2	1015.403	4.3	1820.6477
24	3	25	3	1015.623	2.97	1925.2823	25	1	26	1	1016.0399	7.42	1746.5614
25	2	26	2	1016.3008	5.69	1847.1604	25	3	26	3	1016.5263	-3.55	1952.048
26	1	27	1	1016.9245	10.36	1773.8323	26	2	27	2	1017.192	7.02	1874.7303
27	1	28	1	1017.8026	10.5	1802.1496	27	3	28	3	1018.3141	-3.76	2008.7785
28	1	29	1	1018.6737	4.73	1831.5131	28	2	29	2	1018.9543	5.56	1933.0399
28	3	29	3	1019.1981	-0.65	2038.7425	29	3	30	3	1020.075	-1.48	2069.7716
30	1	31	1	1020.3982	8.18	1893.3772	30	2	31	2	1020.6906	8.04	1995.5731
30	3	31	3	1020.9454	0.57	2101.8653	31	1	32	1	1021.2507	7.79	1925.8773
31	2	32	2	1021.5487	7.73	2028.4226	31	3	32	3	1021.8082	-5.71	2135.0231
32	1	33	1	1022.0968	7.18	1959.4222	32	2	33	2	1022.4	6.23	2062.3266
32	3	33	3	1022.6652	-0.21	2169.2443	33	1	34	1	1022.9365	7.67	1994.0116
33	2	34	2	1023.2442	1.34	2097.2846	33	3	34	3	1023.5146	-3.64	2204.5286
34	1	35	1	1023.7688	-0.7	2029.6452	34	2	35	2	1024.0831	8.54	2133.2963
34	3	35	3	1024.3577	-0.16	2240.8752	35	1	36	1	1024.596	4.29	2066.3225
35	2	36	2	1024.9138	1.8	2170.3611	35	3	36	3	1025.1932	-5.25	2278.2835

**Table 6** continued on next page

**Table 6.** (*continued*)

$J'$	$\Omega'$	$J''$	$\Omega''$	Frequency	Obs-Calc	$E_{\text{lower}}$	$J'$	$\Omega'$	$J''$	$\Omega''$	Frequency	Obs-Calc	$E_{\text{lower}}$
				$\text{cm}^{-1}$	$10^{-4} \text{ cm}^{-1}$	K					$\text{cm}^{-1}$	$10^{-4} \text{ cm}^{-1}$	K
36	1	37	1	1025.4167	8.88	2104.0432	36	2	37	2	1025.739	7.38	2208.4784
36	3	37	3	1026.0229	1.75	2316.753	37	1	38	1	1026.2304	8.71	2142.8069
37	2	38	2	1026.5566	2.92	2247.6478	37	3	38	3	1026.8445	-3.68	2356.283

**Table 7.** Observed transitions for  $^{48}\text{TiO}$ ,  $v = 3 \leftarrow 2$ . Experimental errors for line positions are better than  $1 \times 10^{-3} \text{ cm}^{-1}$ .

$J'$	$\Omega'$	$J''$	$\Omega''$	Frequency	Obs-Calc	$E_{\text{lower}}$	$J'$	$\Omega'$	$J''$	$\Omega''$	Frequency	Obs-Calc	$E_{\text{lower}}$
				$\text{cm}^{-1}$	$10^{-4} \text{ cm}^{-1}$	K					$\text{cm}^{-1}$	$10^{-4} \text{ cm}^{-1}$	K
9	3	8	3	971.8842	-9.69	2642.6613	9	2	8	2	971.9776	-7.06	2540.6435
8	1	7	1	973.1733	-6.69	2433.9371	7	3	6	3	974.1096	-13.7	2624.5381
7	2	6	2	974.1823	5.14	2522.6952	7	1	6	1	974.2611	12.88	2425.5857
6	3	5	3	975.2129	-16.92	2617.0751	6	2	5	2	975.2747	2.39	2515.3042
6	1	5	1	975.341	12.74	2418.2781	5	3	4	3	976.3116	-4.8	2610.6779
5	2	4	2	976.3616	5.66	2508.969	5	1	4	1	976.4151	14.17	2412.0143
3	1	2	1	978.5438	0.37	2402.6183	2	1	1	1	979.5989	-8.14	2399.4863
1	1	2	1	983.7641	2.75	2397.3982	2	1	3	1	984.7904	6.83	2399.4863
3	1	4	1	985.8106	9.41	2402.6183	3	2	4	2	985.8639	-3.71	2499.4657
4	1	5	1	986.8233	-1.92	2406.7943	4	2	5	2	986.8888	-3.93	2503.6894
4	3	5	3	986.9419	-9.26	2605.3468	5	1	6	1	987.8323	10.32	2412.0143
5	2	6	2	987.9078	-1.44	2508.969	5	3	6	3	987.97	-10.75	2610.6779
6	1	7	1	988.8344	14.07	2418.2781	6	2	7	2	988.9211	6.5	2515.3042
6	3	7	3	988.9912	-18.23	2617.0751	7	1	8	1	989.8298	12.42	2425.5857
7	2	8	2	989.9274	7.12	2522.6952	7	3	8	3	990.0074	-10.18	2624.5381
8	1	9	1	990.819	9.11	2433.9371	8	2	9	2	990.9267	1.45	2531.1416

**Table 7** continued on next page

**Table 7.** (*continued*)

$J'$	$\Omega'$	$J''$	$\Omega''$	Frequency	Obs-Calc	$E_{\text{lower}}$	$J'$	$\Omega'$	$J''$	$\Omega''$	Frequency	Obs-Calc	$E_{\text{lower}}$
				$\text{cm}^{-1}$	$10^{-4} \text{ cm}^{-1}$	K					$\text{cm}^{-1}$	$10^{-4} \text{ cm}^{-1}$	K
8	3	9	3	991.0164	-10.2	2633.0669	9	1	10	1	991.8032	18.05	2443.3321
9	2	10	2	991.9204	2.49	2540.6435	9	3	10	3	992.0187	-13.13	2642.6613
10	2	11	2	992.9082	7.21	2551.2007	10	3	11	3	993.0149	-11.59	2653.3212
11	1	12	1	993.751	11.96	2465.2528	11	2	12	2	993.8891	7.23	2562.8129
11	3	12	3	994.0048	-9.35	2665.0464	12	1	13	1	994.716	12.88	2477.7783
12	2	13	2	994.8633	2.99	2575.4802	12	3	13	3	994.9875	-13.14	2677.8366
13	1	14	1	995.6747	11.19	2491.347	13	2	14	2	995.8319	7.33	2589.2022
13	3	14	3	995.9648	-5.71	2691.6917	14	1	15	1	996.6275	13.38	2505.9588
14	2	15	2	996.7938	8.14	2603.9787	14	3	15	3	996.9345	-8.48	2706.6114
15	1	16	1	997.5739	13.48	2521.6136	15	2	16	2	997.7492	7.42	2619.8097
15	3	16	3	997.8975	-12.83	2722.5954	16	1	17	1	998.5139	10.85	2538.3112
16	2	17	2	998.6984	10.13	2636.6947	16	3	17	3	998.8545	-10.98	2739.6435
17	1	18	1	999.4479	10.65	2556.0515	17	3	18	3	999.8047	-11.58	2757.7554
18	1	19	1	1000.3755	9.23	2574.8342	18	2	19	2	1000.5759	-1.87	2673.6262
18	3	19	3	1000.7488	-6.52	2776.9307	19	1	20	1	1001.2971	9.9	2594.6593
19	2	20	2	1001.5057	-0.07	2693.6721	19	3	20	3	1001.6854	-10.32	2797.1692
20	2	21	2	1002.4301	11.56	2714.771	20	3	21	3	1002.6157	-10.48	2818.4705
21	1	22	1	1003.1208	4.75	2637.4354	21	2	22	2	1003.3467	11.57	2736.9227
21	3	22	3	1003.539	-13.73	2840.8341	22	1	23	1	1004.0234	4.33	2660.3861
22	3	23	3	1004.4561	-12.95	2864.2598	23	1	24	1	1004.9202	8.86	2684.3782
23	3	24	3	1005.3685	8.83	2888.7471	24	1	25	1	1005.8104	9.95	2709.4114
24	2	25	2	1006.0573	10.21	2809.691	25	1	26	1	1006.6946	15.54	2735.4857
26	1	27	1	1007.5712	7.8	2762.6006	26	2	27	2	1007.8307	0.54	2863.4607
27	1	28	1	1008.4417	2.54	2790.7558	27	3	28	3	1008.9416	5.78	2997.3041
28	1	29	1	1009.3062	1.94	2819.9512	28	2	29	2	1009.5799	12.19	2921.4327

**Table 7** continued on next page

**Table 7.** (*continued*)

$J'$	$\Omega'$	$J''$	$\Omega''$	Frequency	Obs-Calc	$E_{\text{lower}}$	$J'$	$\Omega'$	$J''$	$\Omega''$	Frequency	Obs-Calc	$E_{\text{lower}}$
				$\text{cm}^{-1}$	$10^{-4} \text{ cm}^{-1}$	K					$\text{cm}^{-1}$	$10^{-4} \text{ cm}^{-1}$	K
28	3	29	3	1009.8168	-6.55	3027.093	29	1	30	1	1010.1643	1.79	2850.1863
29	2	30	2	1010.4435	7.85	2951.9936	30	2	31	2	1011.2999	-1.34	2983.6038
31	1	32	1	1011.8615	2.75	2913.7747	32	2	33	2	1012.9953	5.39	3049.9705
33	1	34	1	1013.5325	1.03	2981.5183							

**Table 8.** Observed transitions for  $^{48}\text{TiO}$ ,  $v = 4 \leftarrow 3$ . Experimental errors for line positions are better than  $1 \times 10^{-3} \text{ cm}^{-1}$ .

$J'$	$\Omega'$	$J''$	$\Omega''$	Frequency	Obs-Calc	$E_{\text{lower}}$	$J'$	$\Omega'$	$J''$	$\Omega''$	Frequency	Obs-Calc	$E_{\text{lower}}$
				$\text{cm}^{-1}$	$10^{-4} \text{ cm}^{-1}$	K					$\text{cm}^{-1}$	$10^{-4} \text{ cm}^{-1}$	K
4	1	5	1	977.5936	12.31	3388.428	4	2	5	2	977.654	-3.24	3485.33
5	2	6	2	978.6653	-13.62	3490.5787	6	1	7	1	979.5879	-15.3	3399.8455
6	2	7	2	979.671	-17.2	3496.8769	6	3	7	3	979.739	-27.27	3598.649
7	2	8	2	980.6717	-7.27	3504.2247	8	1	9	1	981.5629	11.05	3415.4143
9	2	10	2	982.6525	-3.11	3522.0682	10	3	11	3	983.7356	-26.87	3634.6814
11	1	12	1	984.4751	7.24	3446.5494	11	2	12	2	984.607	-8.45	3544.1081
12	1	13	1	985.4325	-3.55	3459.0026	12	2	13	2	985.5751	-5.96	3556.7013
13	1	14	1	986.3852	1.41	3472.4931	13	2	14	2	986.5368	-4.28	3570.3431
14	1	15	1	987.3305	-6.28	3487.0206	14	2	15	2	987.4918	-4.03	3585.0334
15	1	16	1	988.2711	0.96	3502.585	15	2	16	2	988.4402	-6.08	3600.7718
15	3	16	3	988.588	10.65	3703.5467	16	1	17	1	989.2043	-2.53	3519.1862
16	2	17	2	989.3827	-2.71	3617.5581	17	1	18	1	990.1315	-3.27	3536.824
17	2	18	2	990.3183	-3.67	3635.3921	19	1	20	1	991.9673	-4.12	3575.2088
19	2	20	2	992.1699	-5.89	3674.2023	20	1	21	1	992.8761	-0.65	3595.9553
20	2	21	2	993.0868	1.12	3695.1778	21	1	22	1	993.7782	-0.95	3617.7377

**Table 8** *continued on next page*

**Table 8.** (*continued*)

$J'$	$\Omega'$	$J''$	$\Omega''$	Frequency	Obs-Calc	$E_{\text{lower}}$	$J'$	$\Omega'$	$J''$	$\Omega''$	Frequency	Obs-Calc	$E_{\text{lower}}$
				$\text{cm}^{-1}$	$10^{-4} \text{ cm}^{-1}$	K					$\text{cm}^{-1}$	$10^{-4} \text{ cm}^{-1}$	K
21	2	22	2	993.9969	6.42	3717.1999	21	3	22	3	994.1857	-9.31	3821.0872
22	1	23	1	994.6733	-7.68	3640.5557	22	2	23	2	994.8998	5.2	3740.2683
23	1	24	1	995.5633	-2.56	3664.409	23	2	24	2	995.7963	5.09	3764.3825
25	1	26	1	997.3232	-1.17	3715.2208	25	2	26	2	997.5701	11.69	3815.7473
26	1	27	1	998.1931	-5.86	3742.1787	26	2	27	2	998.4452	-3.14	3842.9971
28	2	29	2	1000.1805	16.36	3900.6296	29	1	30	1	1000.766	0.12	3829.2571

**Table 9.** Observed transitions for  $^{46}\text{TiO}$ ,  $v = 1 \leftarrow 0$ . Experimental errors for line positions are better than  $1 \times 10^{-3} \text{ cm}^{-1}$ .

$J'$	$\Omega'$	$J''$	$\Omega''$	Frequency	Obs-Calc	$E_{\text{lower}}$	$J'$	$\Omega'$	$J''$	$\Omega''$	Frequency	Obs-Calc	$E_{\text{lower}}$
				$\text{cm}^{-1}$	$10^{-4} \text{ cm}^{-1}$	K					$\text{cm}^{-1}$	$10^{-4} \text{ cm}^{-1}$	K
29	2	28	2	971.6409	0.7	1401.2293	29	1	28	1	972.0257	13.08	1254.4901
28	2	27	2	972.8882	2.81	1356.2784	28	1	27	1	973.2573	0.28	1210.0286
27	2	26	2	974.1296	3.95	1312.8716	26	2	25	2	975.3644	-3.62	1271.0096
26	1	25	1	975.7062	5.34	1125.6935	25	3	24	3	976.3057	2.83	1381.6879
25	2	24	2	976.5948	3.73	1230.6929	25	1	24	1	976.9209	-2.72	1085.8208
24	2	23	2	977.8185	2.25	1191.9221	24	1	23	1	978.1307	-0.73	1047.4786
23	3	22	3	978.7729	2.54	1304.9548	23	2	22	2	979.0367	3.54	1154.6978
23	1	22	1	979.3348	2.2	1010.6672	22	3	21	3	979.9978	3.54	1268.9298
22	2	21	2	980.2486	1.21	1119.0205	22	1	21	1	980.5327	1.49	975.387
21	3	20	3	981.2163	-0.78	1234.4666	21	2	20	2	981.4552	4.52	1084.8907
21	1	20	1	981.7251	4.69	941.6382	20	3	19	3	982.4295	1.72	1201.5658
20	2	19	2	982.655	-2.01	1052.3089	20	1	19	1	982.9112	3.0	909.4214
19	3	18	3	983.637	6.52	1170.2281	19	2	18	2	983.85	2.54	1021.2755

**Table 9** continued on next page

**Table 9.** (*continued*)

$J'$	$\Omega'$	$J''$	$\Omega''$	Frequency	Obs-Calc	$E_{\text{lower}}$	$J'$	$\Omega'$	$J''$	$\Omega''$	Frequency	Obs-Calc	$E_{\text{lower}}$
							cm <sup>-1</sup>	10 <sup>-4</sup> cm <sup>-1</sup>	K	cm <sup>-1</sup>			
19	1	18	1	984.0917	4.21	878.7367	18	3	17	3	984.8366	-8.77	1140.4538
18	2	17	2	985.0379	-4.18	991.7911	18	1	17	1	985.2661	3.56	849.5844
17	3	16	3	986.033	4.79	1112.2436	17	2	16	2	986.2211	0.5	963.856
17	1	16	1	986.4343	-0.18	821.9649	16	3	15	3	987.2205	-11.18	1085.5979
16	2	15	2	987.3973	-4.36	937.4706	16	1	15	1	987.5971	0.3	795.8784
15	3	14	3	988.4052	5.17	1060.5172	15	2	14	2	988.5684	-1.76	912.6353
14	3	13	3	989.582	2.16	1037.0019	14	2	13	2	989.7333	-0.92	889.3505
14	1	13	1	989.905	2.72	748.3054	13	3	12	3	990.7533	5.89	1015.0525
13	2	12	2	990.892	-2.66	867.6165	13	1	12	1	991.0504	6.58	726.8193
12	3	11	3	991.9184	6.81	994.6692	12	2	11	2	992.0455	3.22	847.4336
12	1	11	1	992.189	2.32	706.8671	11	3	10	3	993.077	4.92	975.8525
11	2	10	2	993.1925	4.42	828.8022	11	1	10	1	993.3223	3.78	688.449
10	3	9	3	994.2299	6.61	958.6028	10	2	9	2	994.3331	2.84	811.7224
10	1	9	1	994.4498	7.09	671.5652	9	3	8	3	995.377	11.87	942.9202
9	2	8	2	995.4684	7.14	796.1945	9	1	8	1	995.571	6.95	656.2157
8	3	7	3	996.5171	8.56	928.8051	8	2	7	2	996.5967	3.18	782.2188
8	1	7	1	996.6866	10.5	642.4008	7	3	6	3	997.6514	8.43	916.2577
7	2	6	2	997.7193	2.04	769.7954	7	1	6	1	997.7956	7.85	630.1206
6	3	5	3	998.7798	11.48	905.2783	6	2	5	2	998.8363	6.47	758.9245
6	1	5	1	998.899	7.98	619.3751	5	3	4	3	999.9004	-1.64	895.867
5	2	4	2	999.9458	-3.22	749.6064	5	1	4	1	999.996	4.68	610.1645
4	3	3	3	1001.0162	-0.09	888.024	4	2	3	2	1001.0511	5.54	741.841
4	1	3	1	1001.0878	9.58	602.4889	3	1	2	1	1002.1727	5.6	596.3484
2	1	1	1	1003.2524	8.43	591.7429	1	1	2	1	1007.5091	5.84	588.6726
2	1	3	1	1008.5581	5.11	591.7429	2	2	3	2	1008.6093	5.33	730.9692

**Table 9** *continued on next page*

**Table 9.** (*continued*)

$J'$	$\Omega'$	$J''$	$\Omega''$	Frequency	Obs-Calc	$E_{\text{lower}}$	$J'$	$\Omega'$	$J''$	$\Omega''$	Frequency	Obs-Calc	$E_{\text{lower}}$
				$\text{cm}^{-1}$	$10^{-4} \text{ cm}^{-1}$	K					$\text{cm}^{-1}$	$10^{-4} \text{ cm}^{-1}$	K
3	1	4	1	1009.6014	7.26	596.3484	3	2	4	2	1009.6637	0.23	735.6286
3	3	4	3	1009.7136	-16.61	881.7494	4	1	5	1	1010.6381	4.91	602.4889
4	2	5	2	1010.7125	1.6	741.841	4	3	5	3	1010.7747	6.48	888.024
5	1	6	1	1011.6692	6.7	610.1645	5	2	6	2	1011.7552	5.01	749.6064
5	3	6	3	1011.8271	6.33	895.867	6	1	7	1	1012.6942	9.54	619.3751
6	2	7	2	1012.7914	5.91	758.9245	6	3	7	3	1012.8734	10.04	905.2783
7	1	8	1	1013.7128	8.02	630.1206	7	2	8	2	1013.8207	0.49	769.7954
7	3	8	3	1013.9126	7.15	916.2577	8	1	9	1	1014.7249	3.97	642.4008
8	2	9	2	1014.8443	2.05	782.2188	8	3	9	3	1014.9448	-0.74	928.8051
9	1	10	1	1015.7313	4.47	656.2157	9	2	10	2	1015.8614	1.96	796.1945
9	3	10	3	1015.9721	6.47	942.9202	10	1	11	1	1016.7316	4.27	671.5652
10	2	11	2	1016.8722	1.29	811.7224	10	3	11	3	1016.9922	7.28	958.6028
11	1	12	1	1017.7258	5.93	688.449	11	2	12	2	1017.8768	3.45	828.8022
12	1	13	1	1018.7136	4.62	706.8671	12	2	13	2	1018.8747	2.19	847.4336
12	3	13	3	1019.0124	5.06	994.6692	13	1	14	1	1019.6956	7.62	726.8193
13	2	14	2	1019.8664	2.2	867.6165	13	3	14	3	1020.0131	7.76	1015.0525
14	1	15	1	1020.671	6.43	748.3054	14	2	15	2	1020.8518	3.68	889.3505
14	3	15	3	1021.0068	6.77	1037.0019	15	1	16	1	1021.6395	-2.01	771.3252
15	2	16	2	1021.8302	-0.35	912.6353	15	3	16	3	1021.9935	1.44	1060.5172
16	1	17	1	1022.6035	6.99	795.8784	16	2	17	2	1022.8026	0.39	937.4706
16	3	17	3	1022.9743	3.7	1085.5979	17	2	18	2	1023.7689	4.8	963.856
17	3	18	3	1023.9481	2.13	1112.2436	18	1	19	1	1024.5105	2.76	849.5844
18	2	19	2	1024.7281	2.86	991.7911	18	3	19	3	1024.9157	5.78	1140.4538
19	1	20	1	1025.4549	3.72	878.7367	19	2	20	2	1025.6812	4.67	1021.2755
19	3	20	3	1025.8763	5.36	1170.2281	20	1	21	1	1026.3931	5.14	909.4214

**Table 9** continued on next page

**Table 9.** (*continued*)

$J'$	$\Omega'$	$J''$	$\Omega''$	Frequency	Obs-Calc	$E_{\text{lower}}$	$J'$	$\Omega'$	$J''$	$\Omega''$	Frequency	Obs-Calc	$E_{\text{lower}}$
				$\text{cm}^{-1}$	$10^{-4} \text{ cm}^{-1}$	K					$\text{cm}^{-1}$	$10^{-4} \text{ cm}^{-1}$	K
20	2	21	2	1026.6274	2.34	1052.3089	20	3	21	3	1026.8298	0.8	1201.5658
21	1	22	1	1027.3246	2.84	941.6382	21	2	22	2	1027.5671	0.78	1084.8907
21	3	22	3	1027.7775	5.77	1234.4666	22	1	23	1	1028.2502	4.18	975.387
22	2	23	2	1028.5004	0.64	1119.0205	22	3	23	3	1028.7173	-0.78	1268.9298
23	1	24	1	1029.1695	6.9	1010.6672	23	2	24	2	1029.4272	1.24	1154.6978
23	3	24	3	1029.6514	3.78	1304.9548	24	1	25	1	1030.0824	7.69	1047.4786
24	2	25	2	1030.3475	2.21	1191.9221	24	3	25	3	1030.5782	1.54	1342.5411
25	1	26	1	1030.9885	5.24	1085.8208	25	2	26	2	1031.261	1.68	1230.6929
25	3	26	3	1031.4987	5.52	1381.6879							

**Table 10.** Observed transitions for  $^{47}\text{TiO}$ ,  $v = 1 \leftarrow 0$ . Experimental errors for line positions are better than  $1 \times 10^{-3} \text{ cm}^{-1}$ .

$J'$	$\Omega'$	$J''$	$\Omega''$	Frequency	Obs-Calc	$E_{\text{lower}}$	$J'$	$\Omega'$	$J''$	$\Omega''$	Frequency	Obs-Calc	$E_{\text{lower}}$
				$\text{cm}^{-1}$	$10^{-4} \text{ cm}^{-1}$	K					$\text{cm}^{-1}$	$10^{-4} \text{ cm}^{-1}$	K
27	3	26	3	971.255	-3.79	1459.3858	27	1	26	1	971.9176	5.07	1161.9564
26	2	25	2	972.7939	-3.72	1266.0184	26	1	25	1	973.1325	11.75	1120.7779
25	3	24	3	973.7306	-8.89	1376.8727	24	3	23	3	974.9599	-8.79	1337.9428
24	2	23	2	975.2332	-4.04	1187.3642	24	1	23	1	975.5455	30.64	1042.9864
23	3	22	3	976.1835	-8.45	1300.5649	23	2	22	2	976.4447	1.26	1150.3438
23	1	22	1	976.7397	3.41	1006.3743	22	3	21	3	977.3999	-20.99	1264.7396
22	2	21	2	977.6503	5.73	1114.8621	22	1	21	1	977.9311	6.66	971.285
21	3	20	3	978.6135	-3.55	1230.4677	21	2	20	2	978.8491	0.44	1080.9193
21	1	20	1	979.1164	6.22	937.719	20	3	19	3	979.8196	-1.96	1197.7495
20	2	19	2	980.0427	1.74	1048.5162	20	1	19	1	980.2961	8.28	905.6765

**Table 10** continued on next page

**Table 10.** (*continued*)

$J'$	$\Omega'$	$J''$	$\Omega''$	Frequency	Obs-Calc	$E_{\text{lower}}$	$J'$	$\Omega'$	$J''$	$\Omega''$	Frequency	Obs-Calc	$E_{\text{lower}}$
				$\text{cm}^{-1}$	$10^{-4} \text{ cm}^{-1}$	K					$\text{cm}^{-1}$	$10^{-4} \text{ cm}^{-1}$	K
19	3	18	3	981.0182	-16.61	1166.5857	19	2	18	2	981.2304	1.6	1017.653
19	1	18	1	981.4697	7.9	875.1578	18	3	17	3	982.2141	0.15	1136.9769
18	2	17	2	982.412	0.1	988.3302	18	1	17	1	982.6374	6.98	846.1633
17	3	16	3	983.4018	-4.7	1108.9236	17	2	16	2	983.5883	3.87	960.5484
17	1	16	1	983.7994	6.86	818.6932	16	3	15	3	984.5846	0.28	1082.4261
16	2	15	2	984.7578	-1.77	934.3078	16	1	15	1	984.955	1.98	792.7478
15	3	14	3	985.7604	-4.86	1057.4851	15	2	14	2	985.9217	-3.59	909.6088
15	1	14	1	986.1057	5.48	768.3273	14	3	13	3	986.9296	-16.08	1034.1009
14	2	13	2	987.0797	-6.33	886.4518	14	1	13	1	987.2489	-6.69	745.432
13	3	12	3	988.0951	-4.62	1012.274	13	2	12	2	988.2324	-1.95	864.8372
13	1	12	1	988.3885	3.8	724.062	12	3	11	3	989.2531	-8.81	992.0047
12	2	11	2	989.3789	-0.21	844.7652	12	1	11	1	989.5213	5.54	704.2176
11	3	10	3	990.4052	-10.93	973.2935	11	2	10	2	990.5193	0.1	826.2361
11	1	10	1	990.648	5.04	685.8989	10	3	9	3	991.5515	-11.61	956.1407
10	2	9	2	991.6545	7.59	809.2503	10	1	9	1	991.7695	10.81	669.1062
9	3	8	3	992.6921	-8.8	940.5467	9	1	8	1	992.8843	9.61	653.8395
8	3	7	3	993.8248	-25.21	926.5118	8	2	7	2	993.905	4.22	779.9093
8	1	7	1	993.9934	9.46	640.0989	7	3	6	3	994.954	-17.41	914.0364
7	2	6	2	995.0213	2.24	767.5546	7	1	6	1	995.0966	10.64	627.8847
6	2	5	2	996.1312	-2.93	756.7441	6	1	5	1	996.1933	5.91	617.1968
5	2	4	2	997.236	0.6	747.478	5	1	4	1	997.2851	12.73	608.0353
4	2	3	2	998.3368	22.44	739.7567	4	1	3	1	998.3703	15.2	600.4003
2	1	3	1	1005.7996	-24.49	589.7082	3	1	4	1	1006.838	-7.81	594.2913
3	2	4	2	1006.8991	15.58	733.5807	4	1	5	1	1007.87	1.48	600.4003
4	2	5	2	1007.943	17.65	739.7567	5	1	6	1	1008.895	0.3	608.0353

**Table 10** continued on next page

**Table 10.** (*continued*)

$J'$	$\Omega'$	$J''$	$\Omega''$	Frequency	Obs-Calc	$E_{\text{lower}}$	$J'$	$\Omega'$	$J''$	$\Omega''$	Frequency	Obs-Calc	$E_{\text{lower}}$
				$\text{cm}^{-1}$	$10^{-4} \text{ cm}^{-1}$	K					$\text{cm}^{-1}$	$10^{-4} \text{ cm}^{-1}$	K
6	1	7	1	1009.9141	-1.69	617.1968	6	2	7	2	1010.0104	10.9	756.7441
7	1	8	1	1010.9274	-0.64	627.8847	7	2	8	2	1011.0345	6.76	767.5546
8	1	9	1	1011.9348	1.99	640.0989	8	2	9	2	1012.0525	5.4	779.9093
8	3	9	3	1012.1524	13.45	926.5118	9	1	10	1	1012.9353	-3.73	653.8395
9	2	10	2	1013.0635	-2.8	793.8079	9	3	10	3	1013.1733	10.52	940.5467
10	1	11	1	1013.9307	0.93	669.1062	10	2	11	2	1014.07	7.32	809.2503
10	3	11	3	1014.1881	10.87	956.1407	11	1	12	1	1014.9192	-2.92	685.8989
11	2	12	2	1015.0688	2.9	826.2361	11	3	12	3	1015.1966	13.17	973.2935
12	1	13	1	1015.9024	1.67	704.2176	12	2	13	2	1016.0619	5.43	844.7652
12	3	13	3	1016.1981	11.17	992.0047	13	1	14	1	1016.879	1.9	724.062
13	2	14	2	1017.0482	3.7	864.8372	13	3	14	3	1017.1927	5.51	1012.274
14	1	15	1	1017.8496	2.76	745.432	14	2	15	2	1018.0288	8.65	886.4518
14	3	15	3	1018.1822	13.93	1034.1009	15	1	16	1	1018.8137	0.92	768.3273
15	2	16	2	1019.0022	4.97	909.6088	15	3	16	3	1019.164	11.76	1057.4851
16	1	17	1	1019.7721	3.47	792.7478	16	2	17	2	1019.9696	5.72	934.3078
16	3	17	3	1020.1394	9.71	1082.4261	17	1	18	1	1020.7241	3.78	818.6932
17	2	18	2	1020.9306	6.34	960.5484	17	3	18	3	1021.108	6.87	1108.9236
18	1	19	1	1021.6691	-3.42	846.1633	18	2	19	2	1021.8848	3.22	988.3302
18	3	19	3	1022.0702	5.47	1136.9769	19	1	20	1	1022.6096	5.68	875.1578
19	2	20	2	1022.8328	2.98	1017.653	19	3	20	3	1023.0257	3.55	1166.5857
20	1	21	1	1023.5421	-2.4	905.6765	20	2	21	2	1023.7743	2.09	1048.5162
20	3	21	3	1023.9751	7.09	1197.7495	21	1	22	1	1024.4693	-0.5	937.719
21	2	22	2	1024.7096	4.02	1080.9193	21	3	22	3	1024.9169	1.74	1230.4677
22	1	23	1	1025.3904	2.47	971.285	22	2	23	2	1025.6384	5.79	1114.8621
22	3	23	3	1025.8532	6.95	1264.7396	23	1	24	1	1026.3048	1.82	1006.3743

**Table 10** *continued on next page*

**Table 10.** (*continued*)

$J'$	$\Omega'$	$J''$	$\Omega''$	Frequency	Obs-Calc	$E_{\text{lower}}$	$J'$	$\Omega'$	$J''$	$\Omega''$	Frequency	Obs-Calc	$E_{\text{lower}}$
				$\text{cm}^{-1}$	$10^{-4} \text{ cm}^{-1}$	K					$\text{cm}^{-1}$	$10^{-4} \text{ cm}^{-1}$	K
23	2	24	2	1026.5603	3.18	1150.3438	23	3	24	3	1026.7816	0.57	1300.5649
24	1	25	1	1027.2126	-2.36	1042.9864	24	2	25	2	1027.4757	1.7	1187.3642
24	3	25	3	1027.7048	9.47	1337.9428	25	1	26	1	1028.1149	1.82	1081.1211
25	2	26	2	1028.3846	-0.13	1225.9225	25	3	26	3	1028.6202	8.19	1376.8727
26	1	27	1	1029.0103	0.3	1120.7779	26	2	27	2	1029.2875	3.85	1266.0184
26	3	27	3	1029.5283	0.17	1417.3539	27	1	28	1	1029.9001	5.67	1161.9564
27	2	28	2	1030.1835	5.17	1307.6511	27	3	28	3	1030.4308	4.89	1459.3858
28	1	29	1	1030.7822	-2.25	1204.6563	28	2	29	2	1031.0725	2.01	1350.8202
28	3	29	3	1031.3258	1.56	1502.9676	29	1	30	1	1031.6593	4.15	1248.8771

**Table 11.** Observed transitions for  $^{49}\text{TiO}$ ,  $v = 1 \leftarrow 0$ . Experimental errors for line positions are better than  $1 \times 10^{-3} \text{ cm}^{-1}$ .

$J'$	$\Omega'$	$J''$	$\Omega''$	Frequency	Obs-Calc	$E_{\text{lower}}$	$J'$	$\Omega'$	$J''$	$\Omega''$	Frequency	Obs-Calc	$E_{\text{lower}}$
				$\text{cm}^{-1}$	$10^{-4} \text{ cm}^{-1}$	K					$\text{cm}^{-1}$	$10^{-4} \text{ cm}^{-1}$	K
22	2	21	2	972.7555	5.92	769.6305	21	2	20	2	973.9413	1.23	746.277
20	3	19	3	974.9027	-10.19	827.7024	20	2	19	2	975.1219	0.83	723.9828
20	1	19	1	975.3693	4.65	624.7359	19	3	18	3	976.0901	-5.62	806.2632
19	2	18	2	976.2964	-2.26	702.7481	18	3	17	3	977.2709	-8.67	785.8939
18	1	17	1	977.6862	10.15	583.7847	17	3	16	3	978.4465	-6.04	766.5946
17	2	16	2	978.6287	-1.93	663.4588	17	1	16	1	978.8355	7.77	564.8824
16	3	15	3	979.6158	-7.05	748.3659	16	2	15	2	979.7861	-2.12	645.4047
16	1	15	1	979.979	4.04	547.0292	15	3	14	3	980.7793	-8.63	731.2079
15	2	14	2	980.9373	-7.15	628.4113	15	1	14	1	981.1166	-0.86	530.2254
14	3	13	3	981.9379	1.01	715.1209	14	2	13	2	982.0837	-1.51	612.4788

**Table 11** continued on next page

**Table 11.** (*continued*)

$J'$	$\Omega'$	$J''$	$\Omega''$	Frequency	Obs-Calc	$E_{\text{lower}}$	$J'$	$\Omega'$	$J''$	$\Omega''$	Frequency	Obs-Calc	$E_{\text{lower}}$
				$\text{cm}^{-1}$	$10^{-4} \text{ cm}^{-1}$	K					$\text{cm}^{-1}$	$10^{-4} \text{ cm}^{-1}$	K
14	1	13	1	982.2496	6.21	514.471	13	3	12	3	983.0885	-12.12	700.1054
13	2	12	2	983.2229	-9.0	597.6075	13	1	12	1	983.3759	4.38	499.7662
12	3	11	3	984.2338	-17.94	686.1615	12	2	11	2	984.3576	-4.31	583.7976
12	1	11	1	984.4966	4.55	486.1111	11	3	10	3	985.3739	-16.67	673.2894
11	2	10	2	985.4859	-4.02	571.0493	11	1	10	1	985.6118	7.7	473.5059
10	3	9	3	986.5073	-24.53	661.4896	10	2	9	2	986.6078	-9.63	559.3628
10	1	9	1	986.7204	2.36	461.9507	9	3	8	3	987.6364	-15.15	650.7622
9	2	8	2	987.7247	-5.53	548.7382	9	1	8	1	987.8242	8.14	451.4455
8	3	7	3	988.7589	-14.14	641.1075	7	3	6	3	989.8753	-16.46	632.5258
7	2	6	2	989.9404	-4.33	530.6757	7	1	6	1	990.0134	9.71	433.5857
6	3	5	3	990.9872	-7.42	625.0176	6	2	5	2	991.039	-7.84	523.2381
6	1	5	1	991.0995	13.58	426.2312	5	3	4	3	992.0848	-89.1	618.5832
5	2	4	2	992.1313	-17.08	516.8632	5	1	4	1	992.179	10.52	419.9269
4	2	3	2	993.2196	-8.86	511.5512	4	1	3	1	993.2536	19.54	414.6729
3	1	2	1	994.3213	19.62	410.469	2	1	3	1	1000.6064	-31.27	407.315
5	1	6	1	1003.6711	-1.62	419.9269	5	2	6	2	1003.7545	11.61	516.8632
6	1	7	1	1004.6798	-4.49	426.2312	6	2	7	2	1004.7746	9.02	523.2381
7	1	8	1	1005.6835	2.49	433.5857	7	2	8	2	1005.7883	4.42	530.6757
8	1	9	1	1006.6809	5.47	441.9905	8	2	9	2	1006.7966	9.27	539.1758
9	1	10	1	1007.6716	1.21	451.4455	9	3	10	3	1007.905	21.88	650.7622
10	1	11	1	1008.6565	-0.82	461.9507	10	2	11	2	1008.7934	5.72	559.3628
11	1	12	1	1009.6362	4.89	473.5059	11	2	12	2	1009.7821	0.8	571.0493
11	3	12	3	1009.9069	12.75	673.2894	12	1	13	1	1010.6087	-0.69	486.1111
12	2	13	2	1010.7652	1.16	583.7976	12	3	13	3	1010.899	16.37	686.1615
13	1	14	1	1011.576	1.82	499.7662	13	2	14	2	1011.7418	0.64	597.6075

**Table 11** continued on next page

**Table 11.** (*continued*)

$J'$	$\Omega'$	$J''$	$\Omega''$	Frequency	Obs-Calc	$E_{\text{lower}}$	$J'$	$\Omega'$	$J''$	$\Omega''$	Frequency	Obs-Calc	$E_{\text{lower}}$
				$\text{cm}^{-1}$	$10^{-4} \text{ cm}^{-1}$	K					$\text{cm}^{-1}$	$10^{-4} \text{ cm}^{-1}$	K
13	3	14	3	1011.8841	14.96	700.1054	14	1	15	1	1012.5368	-0.64	514.471
14	2	15	2	1012.7129	6.91	612.4788	14	3	15	3	1012.8627	12.27	715.1209
15	1	16	1	1013.4917	-0.65	530.2254	15	2	16	2	1013.6768	4.22	628.4113
15	3	16	3	1013.8348	9.69	731.2079	16	1	17	1	1014.4413	6.88	547.0292
16	2	17	2	1014.6345	1.77	645.4047	16	3	17	3	1014.8008	9.83	748.3659
17	1	18	1	1015.3833	-0.94	564.8824	17	2	18	2	1015.5861	2.35	663.4588
17	3	18	3	1015.76	7.16	766.5946	18	1	19	1	1016.3198	-2.79	583.7847
18	2	19	2	1016.5309	-2.1	682.5734	18	3	19	3	1016.7129	7.35	785.8939
19	1	20	1	1017.2504	-1.22	603.7359	19	2	20	2	1017.4703	2.28	702.7481
19	3	20	3	1017.6591	5.32	806.2632	20	1	21	1	1018.1752	1.95	624.7359
20	2	21	2	1018.4022	-3.84	723.9828	20	3	21	3	1018.5991	5.97	827.7024
21	1	22	1	1019.0934	1.79	646.7845	21	2	22	2	1019.3287	-1.0	746.277
21	3	22	3	1019.5326	7.96	850.2109	22	1	23	1	1020.0053	0.02	669.8814
22	2	23	2	1020.2486	0.64	769.6305	22	3	23	3	1020.4589	2.38	873.7884
23	1	24	1	1020.9115	3.04	694.0264	23	2	24	2	1021.1621	1.77	794.0429
23	3	24	3	1021.3789	0.59	898.4346	24	1	25	1	1021.8102	-7.09	719.2194
24	2	25	2	1022.0703	14.55	819.5139	24	3	25	3	1022.2932	8.44	924.149
25	1	26	1	1022.7047	3.75	745.4599	25	2	26	2	1022.9694	0.11	846.0432
25	3	26	3	1023.1997	3.85	950.9312	26	1	27	1	1023.5916	-0.58	772.7479
26	2	27	2	1023.864	5.51	873.6303	26	3	27	3	1024.1001	4.11	978.7807
27	1	28	1	1024.4729	2.45	801.083	27	2	28	2	1024.7511	0.82	902.275
27	3	28	3	1024.9937	3.33	1007.697	28	1	29	1	1025.3472	-1.64	830.465
28	3	29	3	1025.881	6.18	1037.6798	29	3	30	3	1026.7609	1.78	1068.7284
30	1	31	1	1027.0778	-1.97	892.3682	30	2	31	2	1027.3746	-1.85	994.5496
30	3	31	3	1027.635	7.3	1100.8424	31	2	32	2	1028.2364	0.63	1027.42

**Table 11** continued on next page

**Table 11.** (*continued*)

$J'$	$\Omega'$	$J''$	$\Omega''$	Frequency	Obs-Calc	$E_{\text{lower}}$	$J'$	$\Omega'$	$J''$	$\Omega''$	Frequency	Obs-Calc	$E_{\text{lower}}$
				cm <sup>-1</sup>	10 <sup>-4</sup> cm <sup>-1</sup>	K					cm <sup>-1</sup>	10 <sup>-4</sup> cm <sup>-1</sup>	K
32	1	33	1	1028.7833	-1.69	958.4551	32	2	33	2	1029.0915	2.31	1061.3457
32	3	33	3	1029.3617	3.19	1168.2643	33	1	34	1	1029.6274	8.06	993.0666
33	2	34	2	1029.9403	5.69	1096.3263	33	3	34	3	1030.2144	-4.27	1203.5712
34	2	35	2	1030.7822	6.83	1132.3612	34	3	35	3	1031.0616	1.9	1239.9412
35	1	36	1	1031.294	0.97	1065.4239							

**Table 12.** Observed transitions for  ${}^{50}\text{TiO}$ ,  $v = 1 \leftarrow 0$ . Experimental errors for line positions are better than  $1 \times 10^{-3} \text{ cm}^{-1}$ .

$J'$	$\Omega'$	$J''$	$\Omega''$	Frequency	Obs-Calc	$E_{\text{lower}}$	$J'$	$\Omega'$	$J''$	$\Omega''$	Frequency	Obs-Calc	$E_{\text{lower}}$
				cm <sup>-1</sup>	10 <sup>-4</sup> cm <sup>-1</sup>	K					cm <sup>-1</sup>	10 <sup>-4</sup> cm <sup>-1</sup>	K
21	1	20	1	971.8864	5.78	644.3644	20	2	19	2	972.8016	-0.51	721.6488
19	3	18	3	973.767	10.05	804.0225	19	1	18	1	974.2022	3.26	601.5254
18	3	17	3	974.943	20.28	783.7534	18	2	17	2	975.1335	0.48	680.4423
18	1	17	1	975.3515	1.47	581.6713	17	3	16	3	976.1107	5.94	764.549
17	2	16	2	976.2907	-0.46	661.4214	17	1	16	1	976.4951	-0.22	562.8612
16	3	15	3	977.2739	3.64	746.4098	16	1	15	1	977.6338	6.65	545.095
15	3	14	3	978.4313	3.06	729.3361	15	2	14	2	978.5881	-0.09	626.5455
15	1	14	1	978.7658	3.15	528.3731	14	3	13	3	979.5834	7.37	713.328
14	2	13	2	979.7278	-1.97	610.6911	14	1	13	1	979.892	-0.47	512.6955
13	3	12	3	980.7287	1.95	698.3859	13	2	12	2	980.8621	-0.86	595.8925
13	1	12	1	981.0131	1.56	498.0625	12	2	11	2	981.9915	9.42	582.1502
12	1	11	1	982.1282	1.94	484.4741	11	3	10	3	983.0028	3.88	671.7006
11	2	10	2	983.1129	-2.96	569.4642	11	1	10	1	983.2372	-1.65	471.9305
10	3	9	3	984.1316	10.58	659.9579	10	2	9	2	984.2295	-3.45	557.8348

**Table 12** *continued on next page*

**Table 12.** (*continued*)

$J'$	$\Omega'$	$J''$	$\Omega''$	Frequency	Obs-Calc	$E_{\text{lower}}$	$J'$	$\Omega'$	$J''$	$\Omega''$	Frequency	Obs-Calc	$E_{\text{lower}}$
				$\text{cm}^{-1}$	$10^{-4} \text{ cm}^{-1}$	K					$\text{cm}^{-1}$	$10^{-4} \text{ cm}^{-1}$	K
10	1	9	1	984.3412	1.94	460.4318	9	3	8	3	985.2543	16.7	649.2821
9	2	8	2	985.3399	-7.67	547.262	9	1	8	1	985.439	1.84	449.9781
8	3	7	3	986.3695	6.08	639.6733	8	2	7	2	986.4453	-4.34	537.7461
8	1	7	1	986.5306	-2.4	440.5695	7	3	6	3	987.479	-0.82	631.1318
7	2	6	2	987.5442	-5.81	529.2872	7	1	6	1	987.6171	-0.24	432.2061
6	3	5	3	988.5833	0.04	623.6576	6	2	5	2	988.638	-0.16	521.8854
6	1	5	1	988.6971	-5.67	424.8879	5	3	4	3	989.6812	-3.54	617.251
5	2	4	2	989.7255	1.72	515.5408	5	1	4	1	989.7726	3.13	418.6151
4	2	3	2	990.8064	-2.58	510.2535	4	1	3	1	990.8414	2.57	413.3877
3	2	2	2	991.882	-0.75	506.0235	3	1	2	1	991.9048	5.57	409.2057
2	1	3	1	998.1604	6.98	406.0691	2	2	3	2	998.2092	0.31	502.851
3	1	4	1	999.1822	4.79	409.2057	4	1	5	1	1000.1986	6.81	413.3877
4	2	5	2	1000.2697	-1.93	510.2535	4	3	5	3	1000.3286	-4.56	611.9119
5	1	6	1	1001.2089	7.47	418.6151	5	2	6	2	1001.2914	1.28	515.5408
5	3	6	3	1001.36	1.05	617.251	6	1	7	1	1002.2126	1.27	424.8879
6	2	7	2	1002.307	6.06	521.8854	6	3	7	3	1002.3855	9.09	623.6576
7	1	8	1	1003.2109	-0.01	432.2061	7	2	8	2	1003.316	4.42	529.2872
8	1	9	1	1004.2037	4.05	440.5695	8	2	9	2	1004.3184	-0.94	537.7461
8	3	9	3	1004.4157	5.6	639.6733	9	1	10	1	1005.1901	2.51	449.9781
9	2	10	2	1005.3135	-18.78	547.262	9	3	10	3	1005.4208	-1.12	649.2821
10	1	11	1	1006.171	7.05	460.4318	10	2	11	2	1006.306	-0.4	557.8348
10	3	11	3	1006.4207	1.62	659.9579	11	1	12	1	1007.1454	4.55	471.9305
11	2	12	2	1007.2907	1.28	569.4642	11	3	12	3	1007.414	2.66	671.7006
12	1	13	1	1008.1143	7.76	484.4741	12	2	13	2	1008.2692	2.68	582.1502
12	3	13	3	1008.4006	-0.92	684.51	13	1	14	1	1009.0765	4.13	498.0625

**Table 12** continued on next page

**Table 12.** (*continued*)

$J'$	$\Omega'$	$J''$	$\Omega''$	Frequency	Obs-Calc	$E_{\text{lower}}$	$J'$	$\Omega'$	$J''$	$\Omega''$	Frequency	Obs-Calc	$E_{\text{lower}}$
				$\text{cm}^{-1}$	$10^{-4} \text{ cm}^{-1}$	K					$\text{cm}^{-1}$	$10^{-4} \text{ cm}^{-1}$	K
13	2	14	2	1009.2409	-1.49	595.8925	13	3	14	3	1009.3821	9.16	698.3859
14	1	15	1	1010.0326	-0.49	512.6955	14	2	15	2	1010.2068	-0.97	610.6911
14	3	15	3	1010.3561	7.13	713.328	15	1	16	1	1010.9832	0.71	528.3731
15	3	16	3	1011.3222	-9.17	729.3361	16	1	17	1	1011.9282	4.93	545.095
16	2	17	2	1012.1202	0.84	643.4557	16	3	17	3	1012.2847	2.24	746.4098
17	1	18	1	1012.8666	4.28	562.8612	17	2	18	2	1013.0666	-6.95	661.4214
17	3	18	3	1013.2394	-0.45	764.549	18	1	19	1	1013.799	4.35	581.6713
18	2	19	2	1014.0082	0.51	680.4423	18	3	19	3	1014.1881	1.88	783.7534
19	2	20	2	1014.9424	-3.72	700.5182	19	3	20	3	1015.13	0.27	804.0225
20	1	21	1	1015.6455	4.39	622.4232	20	2	21	2	1015.8712	1.11	721.6488
20	3	21	3	1016.0658	2.94	825.356	21	1	22	1	1016.5593	1.66	644.3644
21	2	22	2	1016.7925	-4.85	743.8337	21	3	22	3	1016.995	4.2	847.7537
22	1	23	1	1017.4676	4.17	667.3489	22	2	23	2	1017.7088	1.51	767.0728
22	3	23	3	1017.9177	6.43	871.2151	23	1	24	1	1018.369	0.01	691.3765
23	2	24	2	1018.618	0.72	791.3656	23	3	24	3	1018.8333	1.8	895.7398
24	1	25	1	1019.2649	2.12	716.4468	24	2	25	2	1019.5211	2.85	816.7119
24	3	25	3	1019.7427	1.81	921.3274	25	1	26	1	1020.1545	2.74	742.5598
25	2	26	2	1020.4176	2.78	843.1112	25	3	26	3	1020.6456	1.64	947.9776
26	2	27	2	1021.307	-4.59	870.5632	26	3	27	3	1021.542	2.49	975.6898
27	2	28	2	1022.191	-0.82	899.0675	27	3	28	3	1022.4313	-2.15	1004.4636
28	1	29	1	1022.7856	-1.21	827.1514	28	2	29	2	1023.0676	-7.55	928.6237
28	3	29	3	1023.3141	-5.26	1034.2985	29	1	30	1	1023.6505	0.22	857.432
29	2	30	2	1023.9389	-1.91	959.2314	29	3	30	3	1024.1906	-4.26	1065.194
30	1	31	1	1024.5089	0.31	888.7537	30	2	31	2	1024.8032	-2.38	990.8902
30	3	31	3	1025.0604	-4.52	1097.1497	32	1	33	1	1026.2068	-1.75	954.5195

**Table 13.** Mass-invariant molecular parameters of the  $A^3\Phi$  state of TiO. Two sets of parameters are obtained by excluding (“Fit A”) and including (“Fit B”) the spin-rotation interaction in the electronic ground state (see Table 2). In a global fit, the infrared data obtained in this work are combined with data for  $^{46-50}\text{Ti}^{16}\text{O}$  and  $^{48}\text{Ti}^{18}\text{O}$  at optical and microwave frequencies from the literature (Breier et al. 2019; Lincowski et al. 2016; Fletcher et al. 1993; Ram et al. 1999; Amiot et al. 1995).

Parameter $\hat{O}_{k,l}$	Fit A	Fit B	Units
$U_{00} \times 10^{-4}$	1.41635548(5)	1.41635442(5)	$\text{cm}^{-1}$
$U_{10} \times 10^{-3}$	3.004397(3)	3.004397(3)	$\text{cm}^{-1}\text{u}^{1/2}$
$U_{20} \times 10^{-1}$	-4.5972(5)	-4.5972(5)	$\text{cm}^{-1}\text{u}$
$U_{30} \times 10^1$	-4.88(2)	-4.88(2)	$\text{cm}^{-1}\text{u}^{3/2}$
$U_{01}$	6.084493(4)	6.084491(4)	$\text{cm}^{-1}\text{u}$
$U_{11} \times 10^1$	-1.3146(2)	-1.3145(2)	$\text{cm}^{-1}\text{u}^{3/2}$
$U_{21} \times 10^4$	-9.2(4)	-9.3(4)	$\text{cm}^{-1}\text{u}^2$
$U_{31} \times 10^4$	-1.5(2)	-1.4(2)	$\text{cm}^{-1}\text{u}^{5/2}$
$U_{02} \times 10^5$	9.9762(8)	9.9760(8)	$\text{cm}^{-1}\text{u}^2$
$U_{12} \times 10^7$	6.6(3)	6.8(3)	$\text{cm}^{-1}\text{u}^{5/2}$
$U_{22} \times 10^7$	1.8(3)	1.8(3)	$\text{cm}^{-1}\text{u}^3$
$U_{03} \times 10^{10}$	2.8(2)	2.8(2)	$\text{cm}^{-1}\text{u}^3$
$A_{00} \times 10^{-1}$	5.801031(10)	5.801012(10)	$\text{cm}^{-1}$
$A_{10} \times 10^1$	-3.678(3)	-3.678(3)	$\text{cm}^{-1}\text{u}^{1/2}$
$A_{20} \times 10^2$	1.48(2)	1.48(2)	$\text{cm}^{-1}\text{u}$
$A_{01} \times 10^4$	-5.060(3)	-5.033(5)	$\text{cm}^{-1}\text{u}$
$A_{11} \times 10^5$	1.43(9)	1.30(9)	$\text{cm}^{-1}\text{u}^{3/2}$
$\lambda_{00} \times 10^1$	-5.163(2)	-5.178(2)	$\text{cm}^{-1}$
$\lambda_{10} \times 10^2$	1.12(8)	1.23(8)	$\text{cm}^{-1}\text{u}^{1/2}$
$\lambda_{20} \times 10^3$	-3.5(5)	-3.7(5)	$\text{cm}^{-1}\text{u}$
$\lambda_{01} \times 10^5$	-5.43(8)	-3.74(8)	$\text{cm}^{-1}\text{u}$
$\lambda_{11} \times 10^6$	7(2)	-3(2)	$\text{cm}^{-1}\text{u}^{3/2}$

**Table 14.** Molecular parameters of the  $B^3\Pi$  state of TiO in the singly excited vibrational state  $v = 1$ . All values are given in  $\text{cm}^{-1}$ . Two sets of parameters are obtained by excluding (“Fit A”) and including (“Fit B”) the spin-rotation interaction in the electronic ground state (see Table 2). In a global fit, the infrared data obtained in this work are combined with data for  $^{46-50}\text{Ti}^{16}\text{O}$  and  $^{48}\text{Ti}^{18}\text{O}$  at optical and microwave frequencies from the literature (Breier et al. 2019; Lincowski et al. 2016; Fletcher et al. 1993; Ram et al. 1999; Amiot et al. 1995).

Parameter	Fit A	Fit B
$T \times 10^{-4}$	1.751591015(13)	1.751589964(14)
$B \times 10^1$	5.028657(2)	5.028657(2)
$D \times 10^7$	6.9128(8)	6.9142(9)
$H \times 10^{13}$	1.90(13)	2.02(13)
$A \times 10^{-1}$	2.07884(2)	2.07883(2)
$A_D \times 10^4$	-1.15(2)	-1.14(2)
$\gamma \times 10^2$	2.491(5)	2.490(5)
$\lambda \times 10^1$	-9.305(2)	-9.305(2)
$\lambda_D \times 10^6$	-3.7(6)	-3.8(6)
$\lambda_H \times 10^{10}$	-6.0(1.4)	-5.6(1.4)
$o \times 10^1$	-6.185(2)	-6.184(2)
$o_D \times 10^6$	1.6(4)	1.3(4)
$o_H \times 10^{10}$	5.0(1.0)	6.2(1.0)
$p \times 10^2$	2.6123(8)	2.6121(8)
$p_D \times 10^7$	1.13(3)	1.14(3)
$q \times 10^4$	2.963(3)	2.964(3)
$q_D \times 10^{10}$	-7.2(8)	-8.2(8)